Faculty of Health sciences

Department of Radiology

The Paediatric Wrist; Normal Age Related appearances on Magnetic resonance Imaging and Radiographs.

Follow up of a Healthy Cohort.

—

Derk Frederik Matthäus Avenarius

A dissertation for the degree of Philosophiae Doctor –2017

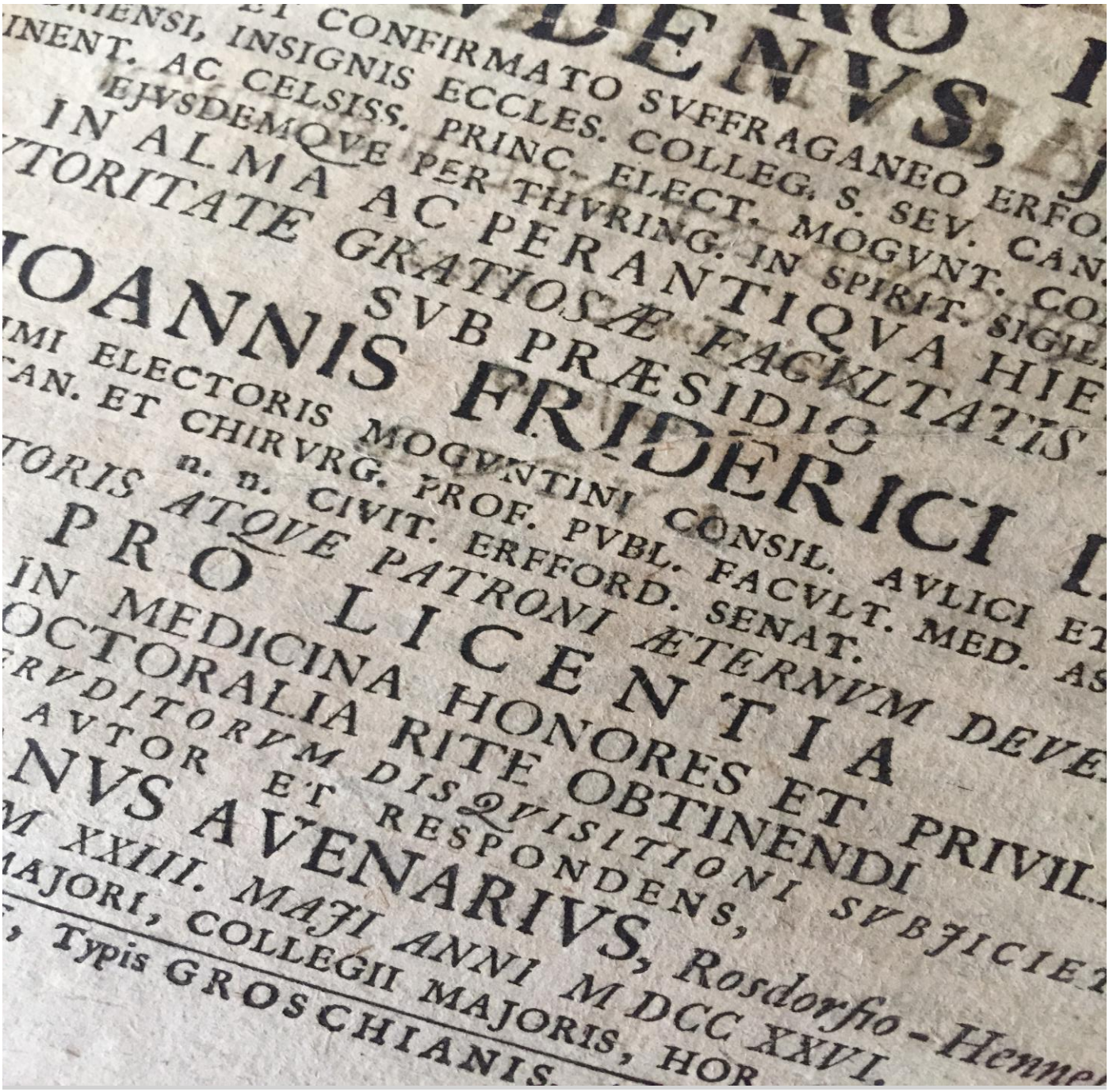

The Paediatric Wrist; Normal Age Related appearances on Magnetic resonance Imaging and Radiographs.

Follow up of a Healthy Cohort.

BY

Derk Frederik Matthäus Avenarius

Institute of Clinical Medicine, University of Tromsø

Department of Radiology, University Hospital of North Norway, Tromsø

2017

Table of Contents

1 Preface

1.1 Scientific environment and work leading up to this thesis

This work has been performed within the Department of Radiology at the University Hospital of Northern Norway (UNN) during the years 2009-2016. The study is founded on collaborative work between the Department of Radiology, UNN, the Department of Surgical Sciences, University of Bergen and the Health-e-Child (HeC) radiology group. The Health-e-Child study involved the collaboration of four large paediatric centres (London, Paris, Rome and Genoa), aiming, amongst others, to devise Magnetic Resonance Imaging (MRI)-scoring systems for involvement of the wrist and hip in children with Juvenile Idiopathic Arthritis (JIA). The study cohort comprised all consecutive patients with JIA with active arthritis in the wrist and/or hip referred to Great Ormond Street Hospital, London/United Kingdom, Hospital Necker Enfants Maladies, Paris/France, Ospedale Gaslini Genoa/Italy, and Ospedale Bambino Gesu, Rome/Italy between October 2006 and 2010; a total of 350 children (200 with wrist involvement). Trying to define MRI-features consistent with active inflammation and destructive changes of the wrist, the researchers noticed wide variations in bone shape, signal intensity of the bone marrow and amount of joint fluid, which in part appeared to be unrelated to disease activity(1).

Thus, to better differentiate disease from potential normal variations, a healthy cohort including 89 children from Tromsø/Norway was examined with MRI and radiographs of the wrist during 2009. The study showed that several of the findings seen in healthy children resembled those found in children with known JIA(2, 3). To better understand the nature of these findings, we performed a follow-up of the healthy cohort after an interval of around four years. For the follow-up we added a specific cartilage-sensitive MR sequence to further characterize the surface of the carpal bones. This thesis includes two papers based on the first analysis of the healthy cohort, and two papers based on the analysis of the follow-up study performed in 2013. The term bone marrow oedema-like change has been used for MRI changes similar to those seen in bone marrow oedema (BMO).

1.2 Acknowledgements

First of all I would like to thank my supervisors Professor Karen Rosendahl, Dr. Lil-Sofie Ording, and Dr. Ellen Nordal for their support and guidance during the work that resulted in this thesis. I would like to express my greatest gratitude to Karen; she has been an excellent mentor and friend, always willing to listen to my ideas, she has taught me to think scientifically and working with her has been a true pleasure. The distance between our institutions has not been a hindrance for a good and fruitful cooperation. I hope that we can continue to work together in our search for the truth. I thank Lil-Sofie for being a great friend, and for her contagious enthusiasm and frequent discussions. Without her drive we would never have started this research. I thank Ellen for her help on the clinical aspects of this thesis and look forward to our continuous cooperation. Through this research I have also been introduced to an enthusiastic group of researchers from other countries and it has been a truly inspiring and scientifically rewarding experience. I would like to thank my international co-authors and especially the Amsterdam group for their Anome initiatives.

None of this would have been possible without all the children that participated and their parents that supported them. I hope they feel that their efforts were worthwhile. I wish to thank the radiographers and other personal in the department that enthusiastically scheduled and performed the examinations, and for the visionary leadership of initially Professor Eldevik, and Professor Norum, and later by Ulf Isaksen and Geir Ingebrigtsen who have supported this research from the start.

I am very lucky to have so many good friends and colleagues on the department of Radiology and I particularly would like to thank Gunnar Oltmanns, Trude Wik, Miguel Castillejo, Christer Amundsen, Torgrim Skiaker, and also Amra Djerzic from the abdominal group who always supported me, and had to put up with my frequent absences. When extra hurdles were put into the path of this, and other work, my colleagues stood by my side, and for that I am very grateful.

Last but not least comes my family, My aunt Petronella, my father Hendrik Amelius and grandfather Derk August have always shown a great interest in my career, and that has been a continues encouragement, they inspired me to start my career in science. I will forever cherish the long weekend meals with its discussions about basic and applied medicine (in Radiology) with my father. He encouraged his children to be curious and observant and taught us about basic principles like Post Hoc, Ergo Propter Hoc already when we were very young. The warmest thoughts go to my caring and loving mother who had to endure all this, and for always supporting me. I am also grateful for the support and interest I have received from my brothers and sisters; I appreciate Hendrik and Johannes for being brothers with exactly the same interests, and my sisters Anna-Maria, Dorothea, and Charlotte for being so different.

Most importantly I have to thank my wonderful children Linn-Emke, Rien, and Ineke for their understanding and acceptance that so much time was spend on this project.
The same is true for my partner in life Veronica who has faithfully stood by my side during the years of this project, and always has been supportive and understanding.

All the drawings and coloured figures in the papers and in this thesis were made in collaboration with the graphical illustrator R. Wollstenholme from the institute of clinical medicine at the University in Tromsø. The coloured drawing of the hands in article 3 was conceived with good help of T. Vangberg from the same institution.

The regional health provider Helse-Nord, has supported this thesis with a six-month research grant.

1.3 List of publications

1. Müller LS, Avenarius D, Damasio B, Eldevik OP, Malattia C, Lambot-Juhan K, Tanturri L, Owens CM, Rosendahl K. The paediatric wrist revisited: redefining MR findings in healthy children. Ann Rheum Dis. 2011 Apr;70(4):605-10.

2. Avenarius DM, Ording Müller LS, Eldevik P, Owens CM, Rosendahl K. The paediatric wrist revisited - findings of bony depressions in healthy children on radiographs compared to MRI. Pediatr Radiol. 2012 Jul;42(7):791-8.

3. Avenarius DF, Ording Müller LS, Rosendahl K. Erosion or normal variant? 4-year MRI follow-up of the wrists in healthy children. Pediatr Radiol. 2016 Mar;46(3):322-30.

4. Avenarius DF, Ording Müller LS, Rosendahl K. Joint fluid, bone marrow oedema like changes and ganglion cysts in the paediatric wrist; features that may mimic pathology. Follow-up of a healthy cohort. AJR Am J Roentgenol. 2017 Mars23:1-6

1.4 Abbreviations

ADC	Apparent Diffusion Coefficient
ANOVA	Analysis Of Variance
ASL	Arterial Spin Labelling
BMO	Bone Marrow Oedema
CNO	Chronic nonbacterial osteomyelitis
CT	Computer Tomography
FID	Free Induction Decay
FSE	Fast Spin Echo
JIA	Juvenile Idiopathic Arthritis
MRI	Magnetic Resonance Imaging
ms	milliseconds
MSK	MusculoSKeletal
mSv	milli Sievert
OMERACT	Outcome Measures in Rheumatology Clinical Trials

PD	Proton Density
PET	Positron Emission Tomography
PVNS	Pigmented VilloNodular Synovitis
RA	Rheumatoid Arthritis
STIR	Short Time Inversion Recovery
TE	Echo Time

1.5 Synopsis

The paediatric skeleton differs from that in adults. We aimed at describing age-related findings of the wrist as assessed by MRI and radiography, particularly findings that might resemble pathology. Following approval from the Regional Ethics Committee, a cohort of 89 healthy children aged 5-15 years was recruited from Tromsø and the surrounding area during 2009. In a first consultation, a radiograph and an MRI of the left wrist were performed. Seventy-four of the children (83.1%) met for a follow-up study during 2013. The initial MRI examination included a T2 weighted fat saturated sequence for assessment of joint fluid and bone marrow oedema-like change and a T1 weighted sequence for depiction of bone shape and bone marrow. The T1 weighted sequence was acquired using thin slices to enable multi-planar reconstruction. The initial examination showed that all children had numerous bony depressions in one or more of the carpal bones, and that these depressions could mimic erosions as defined in the adult rheumatoid arthritis literature(2, 3). Moreover, around half of the children had at least one joint with more than 2 mm joint fluid, as well as bone marrow oedema-like change in at least one of the carpal bones. The comparison of radiography and T1 weighted images revealed a total of 742 bony depressions on MRI as compared to only 95 on radiography.

In sum, the abovementioned MRI findings resembled changes seen in a set of pathological conditions, such as for instance arthritis and trauma. In the 4-year follow-up we repeated the MRI- and radiographic examinations, and also added a cartilage-specific MRI-sequence to better characterize bony depressions. Assuming that damage, or thinning of the cartilage, most likely would preside damage to the underlying bone in children with arthritis, we found it reasonable to believe that bony depressions covered with cartilage most unlikely represent damage, and vice versa, with the exception of sites for ligament insertions.

The four-year follow-up included 74 out of the 89 children examined during 2009; now aged 10-19 years. We assessed and scored bony depressions, bone marrow oedema-like changes and the presence and amount of joint fluid. The results resembled those found during 2009, namely that the number of bony depression increased with age, that around one third had bone marrow oedema like changes in at least one of the carpal bones, and that half had joint fluid pockets deeper than 2 mm. Moreover, bone marrow oedema like changes were found in different areas as compared to the initial examination in 2009, it occurred on both sides of a joint and in close relation to ganglion cysts.

Four out of ten bony depressions were covered by cartilage as assessed on the water-selective-cartilage sequence, with a decreasing percentage by age group. Nearly one third of the uncovered depressions were located at the insertion of the inter-metacarpal ligaments, while the remaining was seen in other juxta-articular areas.

The presence and number of ganglion cysts were examined for both the baseline and the follow-up examinations. One or more ganglion cysts were found in one fourth of the children/adolescents included in both assessments, with six having disappeared during the 4-year period and eleven having appeared.

In conclusion, bony depressions, bone marrow oedema like changes, joint fluid more than 2 mm, and ganglion cysts represent normal findings and should not be interpreted as disease without additional markers for true disease being present. A cartilage-sensitive sequence adds information that might be helpful in differentiating bony surface irregularities during maturation from true destructive changes.

2 Background

2.1 General introduction

Imaging in general and magnetic resonance imaging (MRI) in particular has become exceedingly important in the diagnosis and follow-up of bone disease, allowing for targeted therapy. MRI uses non-ionising radiation, has a high soft-tissue resolution and discrimination and may provide both morphological and functional information. Correct

interpretation depends on extensive knowledge of physical properties and *normal appearances* of the imaged tissue and of the pathophysiological disease processes. Imaging of the paediatric skeleton represents a particular challenge as normal appearances change over time, and may mimic diseases such as juvenile idiopathic arthritis (JIA), osteomyelitis, malignancies and traumatic changes. Potential mimickers include for instance bony surface irregularities, increased marrow signal and joint fluid.

The process of growth and maturation complicates imaging of the skeleton in children, as cartilage ossifies and red marrow converges to yellow. During the enchondral ossification process, the epiphyseal, highly vascular cartilage becomes gradually ossified, replacing the cartilage with bone. Thus, the imaging techniques and the interpretation of findings must be specific to the developmental stage of the child.

To date, the literature on normal standards or references for image based appearances of the wrist in children is sparse. Theodore E. Keats pioneered the field of normal radiographic variations that may simulate disease during the 1960ties – 90ties, with his world-renowned text-books (4, 5) and numerous publications (6-9). He repeatedly underscored the importance of recognizing these entities to avoid errors of commission and diagnosing diseases that do not exist. His observations were, however, based on an extensive experience with reading radiographs rather than population based studies, and with no gold standards available. Moreover, he did not report the prevalence of the different anatomical variations specifically seen in children, such as for example metaphyseal irregularities of the distal radius (8), phalangeal clefts (9), or epiphyseal spurs (10).

In 2011, a MRI scoring system for disease activity and damage in JIA, based on the adult OMERACT (Outcome Measures in Rheumatology Clinical Trials) scoring system, was published(11). Markers for active inflammation were 1) marrow oedema, defined as increased signal on T2 weighted images with a corresponding low signal on T1 weighted images, and 2) synovitis, defined as increased synovial enhancement in up to three wrist compartments, after administration of intravenous contrast. Bony depressions were perceived as erosions. The presence or amount of joint fluid was not included in this particular scoring system.

Others have used joint fluid as a disease marker, both without a defined cut-off between normality and pathology(12-14) and with a defined cut-off (15, 16). For instance, Pierre-Jerome and co-workers, in a study of patients with a negative wrist radiograph after wrist trauma, used a cut-off of 2mm to examine the association between fluid pockets and occult fractures of the wrist (15), while Razek and co-workers used the same cut-off to differentiate between a pathological effusion and normality in the knee joint (16). As for the occurrence of ganglion cysts in children, the literature revealed only one study on symptomatic wrists, reporting a prevalence of around one-third(17).

In adults, Stelling and co-workers have described irregularities at the base of the proximal phalanges mimicking rheumatoid arthritis, based on hand radiographs from 50 healthy adults. These radiographic changes, reported to be an early indicator of rheumatoid arthritis, was seen in at least one site in 10% of the films reviewed(18). Except for our work, similar studies in children are lacking.

As for MRI, a few studies have addressed the appearances of the wrist in healthy adults. One study by Parodi and co-workers, including 23 normal volunteers and using a 0.2 T MR device, showed bone marrow oedema and erosions in 2/23 (8.7%) and in 6/23 (26.1%) subjects, respectively, while tenosynovitis of the extensor tendons was present in 1/23 subjects (4.3%)(19) In 2012, Zwart and colleagues, in a prospective study of 33 healthy volunteers and 60 MRI scans of clinically suspected scaphoid fractures, concluded that MRI was inadequate as a reference standard for true fractures due to a high rate of false positive images (20).

To summarize, the existing literature on imaging appearances of the wrist in healthy children is sparse, and predominately based on small case series and anecdotal reports. This has led to misdiagnosis of a variety of diseases and conditions, such as inflammatory disease, malignancies and traumatic change. In the following the more relevant of these diagnoses will be addressed.

2.2 Diseases and conditions commonly imaged with MRI

The wide spectre of normal findings during maturation of the wrist, with bone surface irregularities, marrow oedema-like change or excessive joint fluid on MRI, may lead to a false diagnosis, particularly if clinical signs and laboratory markers are equivocal. The lack of specific diagnostic tests may typically be the case in juvenile idiopathic arthritis (JIA) and trauma, opposite to septic arthritis, osteomyelitis and malignancies, which can have specific markers. Moreover, incorrect interpretation of normal variants may cause over-estimation of disease activity, distribution, and sequelae in established diagnosis.
The following diseases and conditions may have MRI and/or radiographic findings at the wrist that overlap with the features of healthy children.

2.2.1 Juvenile idiopathic arthritis

Juvenile Idiopathic Arthritis (JIA) is a heterogeneous condition including all forms of chronic arthritis of unknown origin with onset before 16 years of age, and duration more than 6 weeks. It is characterised by chronic synovial inflammation, with potential risk of developing progressive joint destruction and serious functional disability. In the western world it has a yearly incidence of 2-23 cases per 100 000 children under 16 years of age, and a prevalence of 16-170 cases per 100 000(21, 22).

The current classification by the International League of Associations for Rheumatology recognizes seven different categories; oligoarthritis, polyarthritis (rheumatoid factor negative or positive), psoriatic arthritis, enthesitis related arthritis, systemic arthritis and undifferentiated arthritis(23, 24). However, a new classification is discussed, since the categories lack biologic homogeneity, and considerable change in category over time are seen.
The disease is characterized by a lymphocytic proliferation of the synovia. Increased vascularity and permeability of its vessels, and enhanced extravasation of macromolecules and small proteins into the interstitium and ultimately into the joint causing increased joint fluid(25). The proliferation of cells in the subintima causes soft tissue swelling, and this tissue proliferation causes erosions of cartilage and bone by the creation of osteoclasts. The erosions often occur at the attachment points of the synovium, and the destruction of nearby ligaments and bone may lead to joint instability, misalignment, hypertrophy, and luxation. The dysfunctional synovium also leads to cartilage thinning and thus joint space

narrowing, seen on both radiographs and MRI. Osteitis with osteoclasts, mature B-cells, and activated T-cells can occur, and is seen as a precursor for the development of erosions(26). Osteitis is typically seen as an area of high signal on T2 fat suppressed MR images.

Evaluation of joint damage in JIA has traditionally been performed by radiographic scoring methods, including the assessment of bone erosion, cartilage loss (indirectly, through joint space narrowing), and joint misalignment(27). Plain radiographs have, however, a low sensitivity, particularly for disease in early stages(28-31). The method cannot visualize the synovial membrane, joint effusion, articular cartilage or bone marrow directly. On the other hand, MRI is able to image synovitis and bone marrow oedema/inflammation as well as damage to cartilage and bone. MRI can detect erosive changes with greater sensitivity than radiography, particularly in early disease (32). MRI is also capable of detecting tendon pathology and evaluating ligament integrity(28).

2.2.2 Trauma

On MRI, increased marrow signal on T2 weighted images, with a corresponding decreased signal on T1 weighted images is suggestive of bone marrow oedema, which, in a setting of trauma, indicates bone bruise. A coexisting fracture will typically show as a dark line running through the oedema on T2 weighted images. Fractures to the carpal bones in children are rare, but do occasionally occur, most often in the scaphoid bone. MRI has a sensitivity of nearly 100% for the detection of these fractures, however, the specificity is low(33). The existence of pre-traumatic bone marrow oedema-like change as a normal variant might in part explain the low specificity. Overuse and repetitive micro-trauma of the immature skeleton due to exercise and training can result in small avulsion fractures, stress fractures, bone bruise, and widening of the epiphysis with subsequent growth disturbances(34, 35). Rarely, trauma can result in avascular necrosis of a carpal bone while injuries to the ligaments can cause increased joint fluid(33).

2.2.3 Septic arthritis and osteomyelitis

Septic arthritis in children is seen in 2-13 per 100 000 per year in developed countries, can affect one or more joints and warrants a prompt diagnosis and treatment to reduce the

risk of complications(36). It is often associated with osteomyelitis, which, on MRI, shows as high signal on T2 weighted images, and subsequently as destructive change on radiographs(37). An infected joint is characterized by effusion, soft tissue swelling, synovial hypertrophy, loss of cartilage, osteoporosis, and, in some cases, by bone destruction(38). In most cases, clinical symptoms, laboratory findings and a joint puncture in cases of mono arthritis will secure the diagnosis. However, occasionally the findings may overlap with those of normal variation, e.g. joint fluid, bone marrow oedema-like change and bony depressions. Rarely recurrent synovitis can be caused by the presence of foreign bodies (39).

2.2.4 Chronic nonbacterial osteomyelitis

Chronic nonbacterial osteomyelitis (CNO) may present with symptoms and signs suggestive of osteomyelitis and/or arthritis. CNO is a bone disorder of unknown cause, primarily occurring in children and adolescents. It is characterized by pain and swelling of the involved bones, and is predominantly located in the metaphysis. The tibia, clavicle, pelvis, fibula, distal radius, and femur are most often affected; rarely also metacarpal bones can be involved in this disease(40). The disease is almost always multifocal and symmetric involvement is common. The radiographic and MRI characteristics resemble osteomyelitis, with its high signal on T2 weighted images, but without the formation of abscesses and fistulas. Lesions in close proximity to the joint can give arthritis-like symptoms, with joint swelling and increased joint fluid. Typically, the disease has a prolonged course with flares over many years(41, 42).

2.2.5 Transient synovitis

Transient synovitis is characterized by joint effusion, synovial hypertrophy and pain. Its cause is unknown, although it is thought to represent a post-infection reactive arthritis, and although most commonly seen in the hip, other joints including the wrist, may be involved (43, 44).

2.2.6 Haemophilic arthropathy

Haemophilia is a rare, X-linked, inherited bleeding disorder; it is a disturbance of the coagulation cascade caused by a deficiency of clothing factor VIII or IX. Joints are affected by intra articular bleedings in around 90% of patients with severe disease, mostly in the knees, ankles, hips elbows and shoulders, but the joints of the hand can also be affected(45). These bleedings can occur at age 2-3 years and may result in haemophilic arthropathy; a self-perpetuating cycle of haemarthrosis-synovitis-haemarthrosis(46). The exact mechanism behind the arthropathy is not known, but is most likely multifactorial. The synovial changes precede the cartilage changes, and some suggest that the intraarticular blood has a direct detrimental effect on cartilage as a result of the iron-catalysed formation of destructive oxygen metabolites, subsequently affecting the synovium. Others suggest that there is a haemosiderin-induced synovial triggering process(47). On radiography the disease is visible as subchondral cysts and bone deformities, other signs of the disease such as cartilage loss, synovial swelling, joint effusion, erosion, haemosiderin deposition and periarticular oedema are seen indirectly. The hyperaemia of the synovium can induce hypertrophy of the bones in the affected joints. With MRI the soft tissue are well visualised, and MRI with T2* weighted sequences demonstrating intra articular iron can even be diagnostic. MR imaging can also be used for follow-up or as a tool to visualize preclinical pathology (47, 48).

2.2.7 Pigmented villonodular synovitis

Pigmented villonodular synovitis (PVNS) is a relatively rare, mostly benign hypertrophic synovial process characterized by villous, nodular, and villonodular proliferation with pigmentation from haemosiderin. The exact composition of these elements varies from lesion to lesion. PVNS can affect the synovium of the joint, the tendon sheath or the bursa. It can be monoarticular or affect multiple joints; it can be focal or diffuse. Although more common in adults, it is also seen in children. Radiographs are mostly normal or only show a localized soft tissue swelling. In case of a diffuse intraarticular form of PVNS, extrinsic erosions of bone on both sides of the joint can be seen on the radiograph. Periosteal reactions or calcifications can sometimes be seen in case of tendon sheath affection. Most of the other features like joint fluid, synovial and soft tissue affection and extension are best visualised on MRI. The pigmentation by iron deposits can be shown with T2* weighted sequences similar to the ones used for haemophilic

arthropathy. Other MR imaging findings are bone erosions, subchondral cysts, bone marrow oedema, and articulocartilaginous defects(49, 50). Although there is an overlap with bony depressions, joint fluid, and bone marrow oedema-like change seen in normal variants for PVNS and haemophilic arthropathy this is rarely a problem due to clinical information and the imaging features of the iron deposits.

2.2.8 Synovial chondromatosis

Chondromatosis involves the synovium, with hypertrophy and multiple nodular projections of hyaline cartilage that may extend outside the joint and cause bone erosions. It is primarily seen in adults, may occur in children, but only rarely affects the wrist (51). Radiographs are normal in 5-30%. MRI shows synovial hypertrophy, and the hyaline cartilage nodules have high signal on T2 weighted images and may resemble fluid pockets(52).

2.2.9 Synovial haemangioma

Synovial haemangioma is a congenital angiodysplastic malformation that can give a mass effect with limitation of motion and pain. It can occasionally bleed into the joint and give the same symptoms and radiological signs as haemophilic arthropathy. It is recognized on imaging by its vessels(38). Sometimes the mass effect is not pronounced, and hemangiomas can then be difficult to differentiate from infectious or reactive arthritis(53).

2.2.10 Malignancy

Leukemic arthritis can occur due to infiltration of the synovium and haemorrhage into the joint or soft tissue around the joint. These changes may precede changes in peripheral blood counts by weeks and months. Distinct metaphyseal bands of demineralization adjacent to the growth plate are nonspecific, but highly suspicious for leukemia. Other radiographic findings include osteopenia, erosions, osteolytic lesions, and cortical lesions(38). Other childhood malignancies like neuroblastoma, lymphoma, malignant

histiocytosis, rhabdomyosarcoma and diseases like sarcoidosis and eosinophilic granuloma, may give symptoms that mimic arthritis, with MRI findings consistent with bone marrow oedema. However, there is normally no involvement of the synovium(38, 56).

2.2.11 Miscellaneous

The complete list of differential diagnosis is long as many rare conditions may involve joints and present with overlapping symptoms and radiological findings. In rare cases, osteoid osteoma can be seen in a carpal bone, with joint fluid, bone marrow oedema, sclerosis, soft tissue swelling, pain and a nidus that can resemble an erosion(54). Chondroblastoma, a rare tumor of the epi- and apophysis, may be located near the joint space and seen radiographically as a lytic lesion resembling an erosion. The prostaglandin production of this tumour produces bone marrow oedema, increased joint fluid, and soft tissue swelling(55).

3 The wrist

3.1 Development of the hand

The hand starts to develop during early stages of foetal growth, though chondrification and ossification to finally achieve skeletal maturity at the end of adolescence(57). Enchondral ossification of the carpal bones begins at around three months of age with the capitate bone and ending with the pisiform bone(58). In most children, bone growth and modeling follows a specific sequential pattern with a constant ratio between carpal bone volumes (59, 60). Radiographically, the small spherical ossification centers develop into multifaceted, articulating bones with a well-defined cortex. With growth, the bony surface may take a slightly more squared and irregular form, the three-dimensional nature of which is better appreciated on MR images than on radiographs.

The carpal bones ossify in a relatively ordered fashion; beginning with the capitate and then making a circle to the hamate, triquetral, lunate, scaphoid, trapezium, and ending with the trapezoid bone. The pisiform bone is special in that is ossifies much later at around 7-9

years in girls and around 9-11years in boys. The capitate ossifies at around 1-3 months just before the hamate at 2-4 months. The triquetral bone starts to ossify at around 2-3 years and the circle ends with the trapezoideum that ossifies at 4-6 years. The distal radius ossification centre appears at around 1 year and the ulnar ossification centre first at around 5-6 years of age. The scaphoid ossification usually appears before that of the trapezium in boys and either just before or just after in girls, the ossification of both occurs by three years(57). The ossification centres normally appear earlier in girls than in boys with the biggest difference in the last appearing centre; the pisiform bone that can appear a few years earlier in girls. The epiphyses of the metacarpal bones appear on radiographs beginning with the second metacarpal bone at 1.5 years, followed by the third, fourth, fifth, and ending with the first metacarpal bone at around 5 years of age(61).

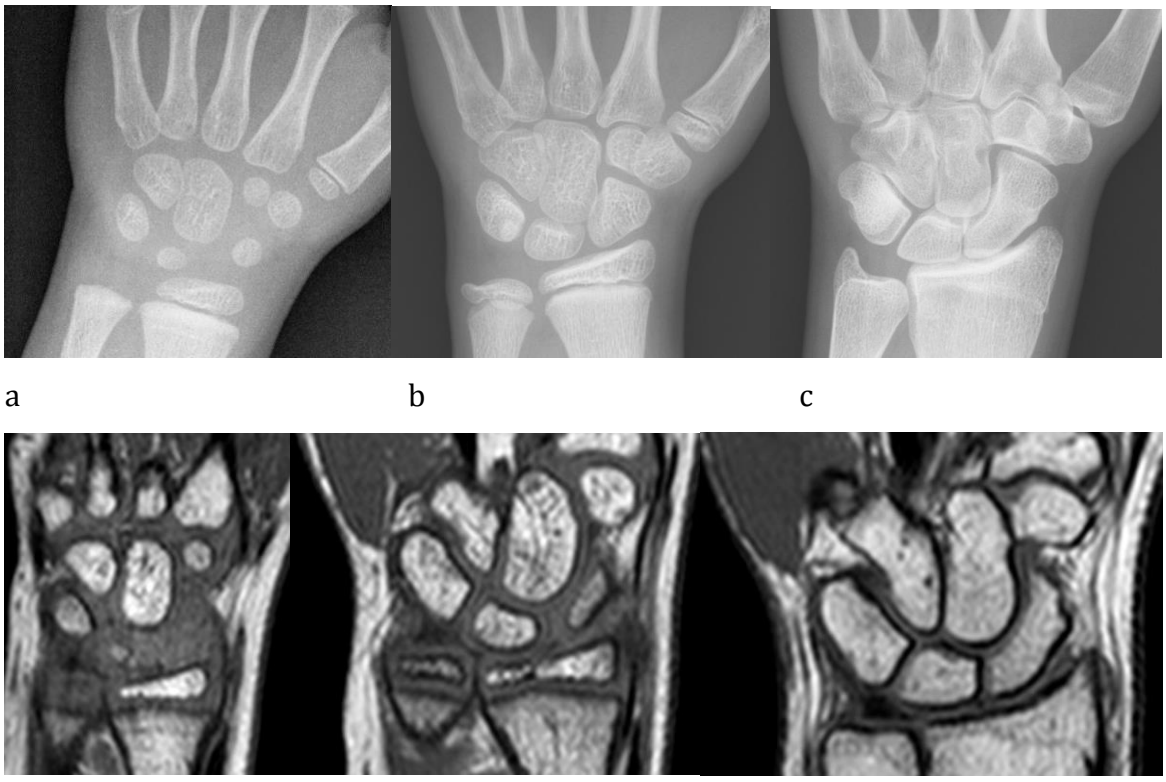

a b c

a b c

Figure 3.1 Radiograph and corresponding T1 weighted MR image at 6 years (a), 10 years (b), and at 17 years(c) of age in three different, healthy girls.

3.2 Synovium

The synovium is the soft tissue lining the spaces of the diarthrodial joints (except for the cartilage), the tendon sheets, and the bursae. It consists of a continuous surface layer (intima) of cells and the underlying tissue (subintima). It does not have a basal lamina. The intima cells are derived from macrophages and mostly fibroblasts lineage, while the subintima includes blood and lymphatic vessels, a cellular content of both resident fibroblasts and infiltrating cells in a collagenous extracellular matrix(62), with nerve fibres, including sympathetic nerves around the blood vessels. There are three different types of subintimal layer, namely a fibrous, an areolar with multiple layers of lining cells for stretching and folding, and an adipose (figure 3.2).

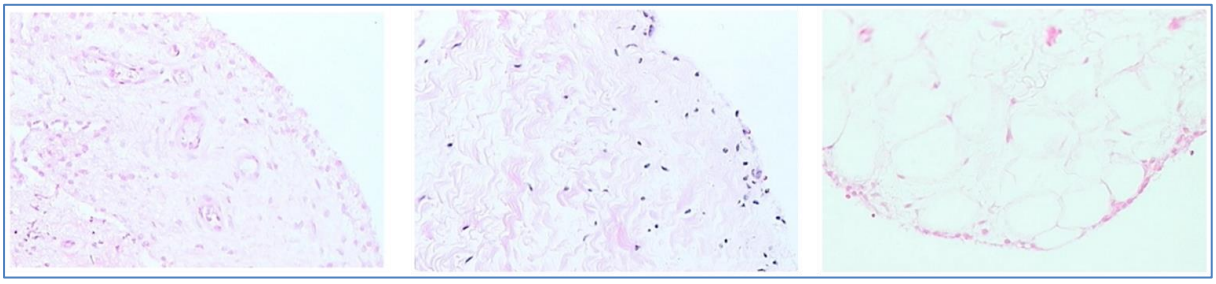

a b c

Figure 3.2 The three different types of subintima; a) areolar, b) fibrous and c) adipose type (H+E-stain). *Images from "The Normal Synovium "© Malcolm D. Smith; Licensee Bentham Open.*

The sub-intimal matrix is an amorphous, fine, fibrillar ultrastructure containing collagens, proteoglycans, fibrillin-1, and hyaluronan. In addition to several different lymphoid cells, this layer contains fibroblasts, osteoblasts, chondrocytes, and fat cells. The function of the normal synovium is to provide a deformable packing and facilitate movement of underlying non-deformable tissues(62). The production of hyaluronan by intimal fibroblast is thought to be important for inhibiting adhesion fibrin formation and scarring. This substance is also important in maintaining a film of lubricant on the cartilage surfaces and is probably the main factor responsible for retaining a constant volume of fluid during exercise(63). The synovium is also a major route of nutrition for chondrocytes; even in major joints the synovial folds are often not further away than 50mm from the cartilage. The subchondral plate is incomplete in children and may contribute to nutrition in this age group.

Image-wise, the normal synovium is visible on ultrasound and MRI, but not on radiographs. On ultrasound, it appears as a hypo-echogenic layer with a varying thickness according to type (figure 3.3).

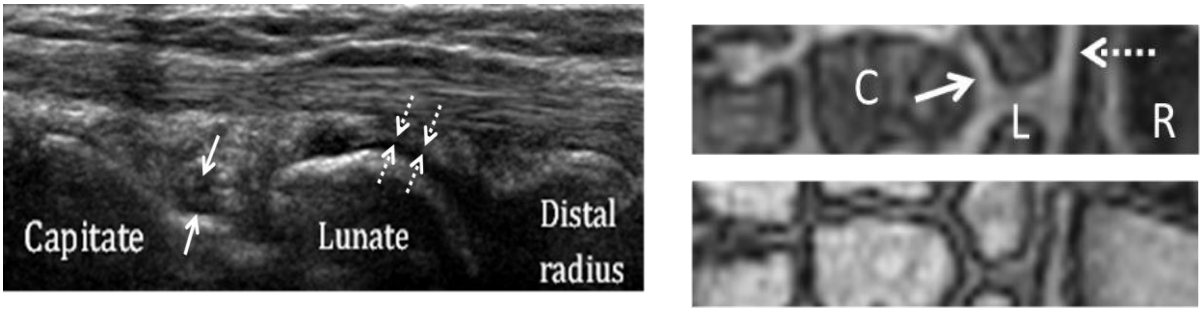

a b

Figure 3.3 showing a) sagittal ultrasound image of the dorsal wrist and b) coronal MR-images (T1 weighted images before (bottom) and after intravenous contrast administration). Normal synovium in the midcarpal joints (arrows) and in the radiocarpal joints (stippled arrows). R=radius, L=lunate, C=capitate.

3.3 Joint fluid

Joint fluid is produced by fenestrated sub-intimal small vessels as an ultra-filtrate of blood plasma(63), enriched and maintained by the synovium intima cells of fibroblast lineage. These contain a large endoplasmatic reticulum for the production of hyaluronan and many other compounds found in synovial fluid, such as collagenase, plasminogen activator, decay-accelerating factor, and prostaglandins. The addition of these proteins to the plasma inhibits fibrin formation and scarring and gives it its typical viscosity(62). The intima cells of macrophage linage are filled with lysosomes for removal of waste products from the synovial fluid, and the lymphatic vessels of the intima helps maintaining a constant flow through the fluid thus facilitating oxygenation and nutrition of the cartilage, and the deportation of waste products. The ability to lubricate articular surfaces is dependent on the production of a glycoprotein known as lubricin found on the surfaces of cartilage and synovium(64), it is produced by intimal fibroblasts and chondrocytes. The hyaluronan is probably important to maintain a film of lubricant on the surface of the articular cartilage, and to maintain a constant volume under exercise when the intra articular pressure increases due to repeated flection(63). Its production is probably

regulated by the mechanical stress on the fibroblasts(62). The production of fluid seems to be increased after exercise and with increased temperature as this increases the distribution rate of gadolinium contrasts into the joint space(65).

Fluid in joint spaces in the wrist can be found in the different compartments that are separated from each other by the intrinsic ligaments of the wrist(66). The wrist is divided into seven standard compartments, from proximal to distal in three areas that normally do not communicate with one another, but normal variation may occur (figure 3.4):

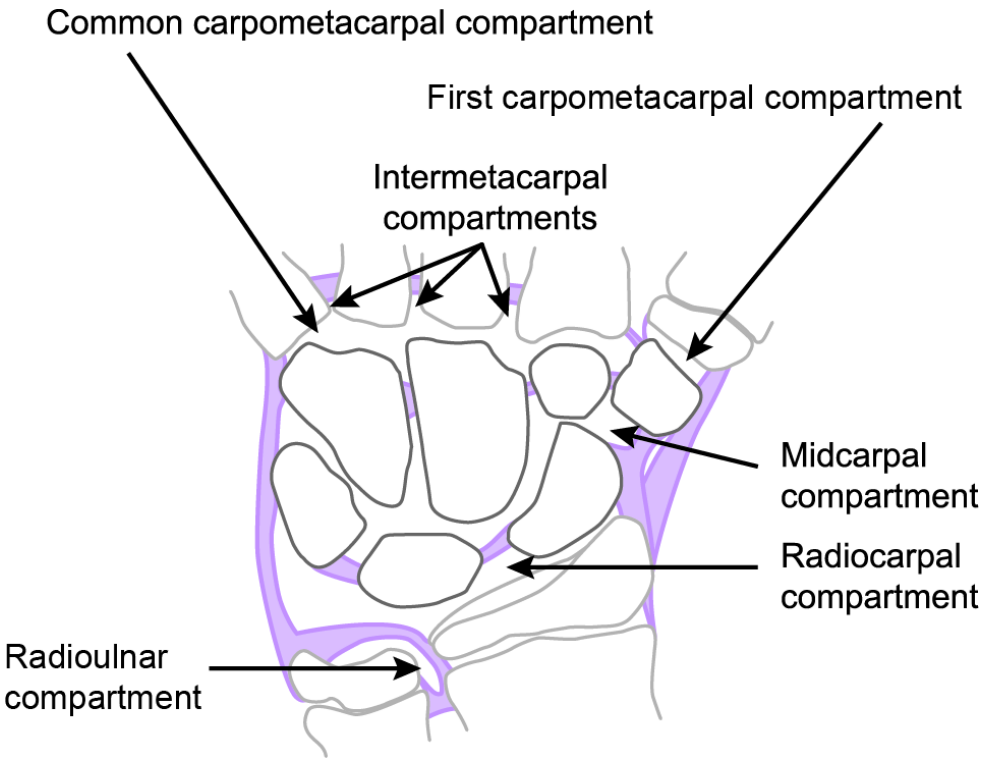

Figure 3.4 Compartments of the wrist: ***Area 1****: the radioulnar compartment, separated from the radiocarpal compartment by the triangular fibrocartilage,* ***Area 2****: the radiocarpal compartment between the proximal carpal row and the distal radius and triangular fibrocartilage, the pisiform-triquetral compartment that communicates with the radiocarpal joint in around 80% of cases(67) (not shown in this figure) and* ***Area 3*** *in which there normally is communication: the midcarpal compartment, including the space between the scaphoid and the trapezial bones, the common carpometacarpal compartment between the distal carpal row and the base of metacarpal bones 2-5, the first carpometacarpal*

compartment and the intermetacarpal compartments between the bases of the metacarpal bones 2-5.

There is a tendency to increased communication between the compartments with age due to degeneration of the natural boundaries like ligaments and the triangular cartilage.
On imaging, joint fluid is visible on MRI and on ultrasound (figure 3.5).

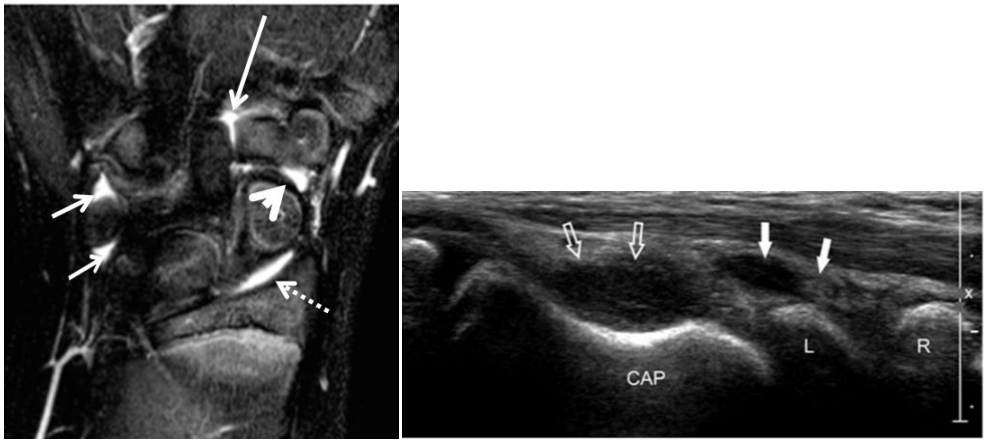

a b

Figure 3.5 a) Coronal T2 weighted MR image of the wrist in a healthy 14-year old boy, showing joint fluid in Area 2 (the radiocarpal (stippled arrow) and the pisiform-triquetral (short arrows) compartments) and Area 3 (the midcarpal compartment (arrowhead) and common carpometacarpal compartment (long arrow)), b) sagittal ultrasound image of the dorsal (extended) wrist in a healthy 14 year old, showing fluid in the radiocarpal compartment (arrows) and in the midcarpal compartment (open arrows). CAP=capitate, L=lunate, R=radius.

3.4 Ganglion cysts

Ganglion cysts are the most common lesion seen in the wrist and ankle, and are common benign features in adults. They are surrounded by a thin capsule, vary in size from only a few mm up to 5 cm and have varying consistency depending on its internal pressure. Different treatment options do exist like surgical excision, aspiration, corticoid injection, or anti-inflammatory medication. Doing nothing is also an option as spontaneous remission does occur. Ganglion cysts have a thin connective tissue capsule and in the wrist,

they are commonly seen on both the dorsal and on the palmar-radial aspects(68). The aetiology is unclear (69, 70), however, current hypotheses include myxoid degeneration of the collagen fibres and post-traumatic synovial/capsular and ligament irritation with secondary production of hyaluronan. Direct extension from the joint is less likely because of the lack of synovial lining of the cyst wall, although it is possible that this synovial lining could have degenerated. The walls consist of collagen fibres with no cellular epithelial lining(71), and it has been postulated that joint capsules and/or ligaments produce mucin as a reaction to stress, which in turn stimulates the production of modified synovial cells or fibroblasts. The mucin then dissects through the ligamentous and capsular structures with eventual coalescence into a cyst(17). The cyst may dissect into the bone as intra osseous cysts, or into ligaments, tendons or even nerve sheets as intra neural ganglion cysts. It has been shown, using intra-articular administration of contrast media, that ganglia may have a direct connection to the joint, and that valve mechanisms can exist in the connecting stalk, giving rise to the fluid filled structure. Ganglia have been reported at all ages, with the dorsal ganglia more common in the second to fourth decade and the volar more common in the fifth to seventh decades(72). In a series of 103 asymptomatic adult volunteers aged 18 to 75 years, Lowden and co-workers identified ganglia in 51% of the wrists, of which 70% originated from the palmar capsule(68).

Image-wise, ganglion cysts are visible on MRI and on ultrasound (figure 3.6). On ultrasound, they appear as round or oval, well circumscribed anechoic lesions, and on MRI they return high signal on T2 weighted images.

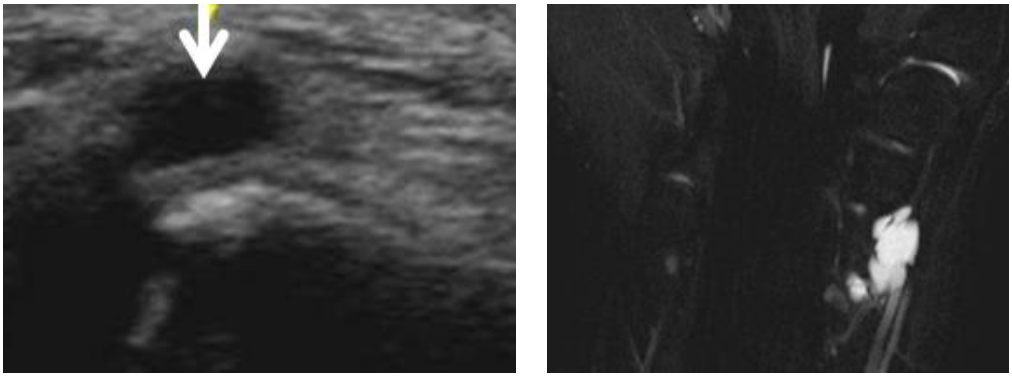

a) b)

Figure 3.6 a) Ultrasound of the wrist in a healthy 8 year old girl, showing a round, anechoic lesion adjacent to the midcarpal joint, consistent with a ganglion (arrow) and b) coronal T2 weighted fat suppressed MR image of the wrist in a 14 year old girl, showing an irregular, hyper intense lesion near the radiocarpal joint.

3.5 Cartilage

Articular cartilage is an avascular, complex, specialized tissue covering and protecting the bone ends at joints. It is composed of chondrocytes that produce extracellular matrix consisting of proteoglycans around a network of collagen fibres, organized in multiple arcs. Nutrition and oxygenation of the articular cartilage and underlying bone is mainly supplied by diffusion from the synovium through the joint fluid(73).

Hyaline cartilage in the epiphyses and carpal bones differs from articular cartilage in that it is penetrated by vessels, the collagen fibrils are thicker and more uniformly orientated, it contains more chondrocytes and the extracellular matrix is rich in collagen, glycosaminoglycans and other non-collagenous proteins(74). Glycosaminoglycans are highly polar mucho-polysaccharides that attract water and can be used as lubricants or shock absorbers. Hyaline cartilage mainly consists of water of which most is bound to collagen(75). Before ossification the chondrocytes hypertrophies (74) and the vascular canals merge into discrete networks, releasing metalloproteinases like gelatinase B and collagenase-3. The cartilaginous matrix dissolves, water content increases, and ossification occurs. At first, the ossification centre contains hematopoietic red marrow.. After around 6 months, red marrow is replaced by yellow marrow although patches of red marrow may persist for longer(76).

On MRI, due to a higher content of free (not bound to macromolecules) water, articular cartilage returns a slightly higher T2 signal than does the epiphyseal- or hyaline cartilage. Macromolecules like collagen and glycosaminoglycan in epiphyseal cartilage have a strong binding to water molecules and this result in lower intensities on T2 weighted images. The ossification process starts with the degradation of macromolecules within cartilage, and subsequent release of the bound water. This can lead to areas with high signal on T2 weighted fat suppressed images, which is known to occur in the humerus and in the knee(77, 78). The MR signal of cartilage is therefore very different depending on the state of maturation or function (articular versus epiphyseal).

Image-wise, cartilage is visualized directly on ultrasound and MRI, and indirectly on radiographs (figure 3.7).

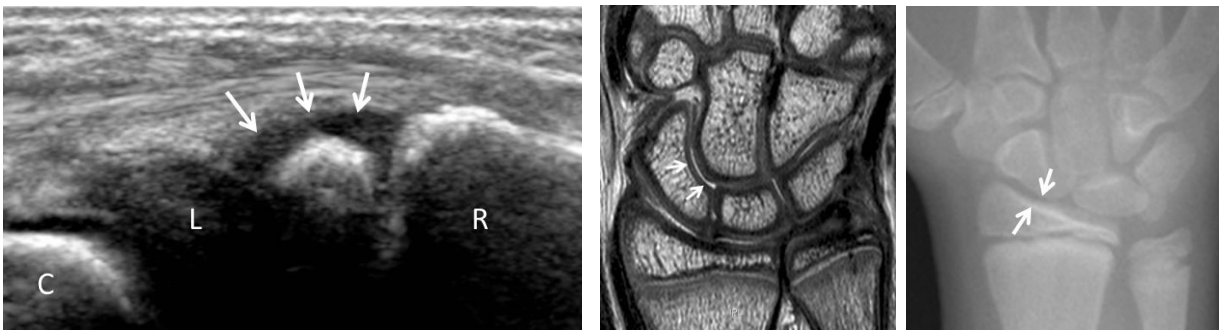

a) b) c)

Figure 3.7 a) Sagittal ultrasound image in a 3 year old, healthy girl, showing a dark zone adjacent to the distal radius epiphysis (arrows), consistent with cartilage, b) coronal, proton weighted MR image in a healthy 14 year old showing the carpal bones surrounded by a grey zone of cartilage (arrows) and c) radiograph of the wrist in a 14 year old. The dark zone between the bones represents two layers of cartilage (arrows).

3.6 Tendons and ligaments

Tendons and ligaments consist of dense, regular networks of collagen fibres (86%), elastin (2%), and 1-5% proteoglycans. Collagen fibres are built up from smaller collagen molecules to form fibrils, then fascicles, to tendon fibres. The collagen is produced by an interconnected network of tenocytes, that has the possibility to respond to mechanical load(79). The connective tissue of the endotendineum surrounds the fascicles, which are formed to bundles surrounded by the epitendon. The outer layer of the tendon is the fatty areolar tissue of the paratendon, with its nerves and vessels branching into the epitendon, with vessels, in contrast to nerves, also having branches into the endotendineum. Where tendons pass under ligaments or through osseo-fibrous tunnels that could give friction, like the many tendons in the wrist and ankle, one can find the synovial sheath that facilitates this movement. The tendon sheath is a synovial lining of the tendon, the fibrous tendon sheath is the outer membrane of a structure that invaginates the tendon to form a double layer filled with synovial fluid for friction reduction. This double structure is interrupted at its connection by the mesotendon, allowing blood vessels and nerves to reach the tendon.

3.7 Bone marrow

Generally there are two types of bone marrow; the red hematopoietic active bone marrow with a fat content of 40%, and the yellow bone marrow that contains 80% fat. In adults, red bone marrow is found in the flat bones like ribs, pelvis, scapula and in the vertebrae, but also in the proximal metaphysis of the femur and humerus. At birth, red marrow fills all the marrow cavities. During growth this is slowly replaced with yellow bone marrow at a predictable rate and pattern that reaches its final distribution at age 25. Yellow bone marrow can reconvert to red bone marrow under certain circumstances that require an increase in red or white blood cells, like chronic blood loss, infections, or malignancies. Obesity, smoking, diabetes and exercise are also reasons for reconversion. The cartilage in the carpal bones develops into the secondary ossification centre via an organized degradation of the cartilage and its chondrocytes with an increased vascularization and osteoblast activation. After ossification it takes about 6 months to convert the red marrow to yellow marrow but patches of red marrow can persist for a longer period(76). MRI is the only modality visualizing bone marrow (figure 3.8).

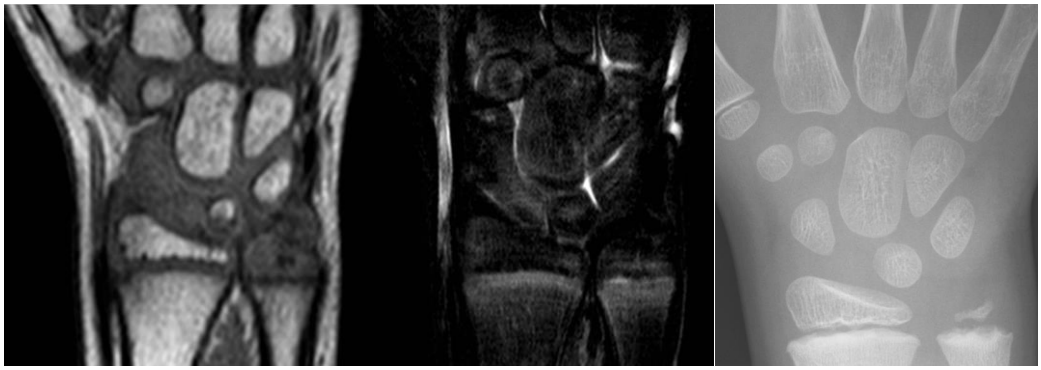

a b c

Figure 3.8 Bone marrow as assessed on MRI in a healthy 7-year-old boy a) T1 weighted image showing yellow bone marrow (high signal), b) fat suppressed T2 weighted image showing red bone marrow in the metaphysis of the radius and ulna (high signal), and c) a corresponding radiograph.

4 Radiological methods used in this thesis

Current imaging methods for diagnosing bone pathology include radiography, ultrasound, magnetic resonance (MRI), computed tomography (CT) and positron emission tomography (PET). Most methods use electromagnetic radiation to form images; radiography and CT from the ionizing spectre, and MRI from the non-ionizing spectre. Ultrasound uses short pressure pulses. In the following I will focus on radiography and MRI, which are the modalities used in this thesis.

4.1 Radiography

Radiography is the oldest medical imaging technique and was discovered in 1895 by Wilhelm Konrad Röntgen. X-rays are produced when fast moving electrons decelerate and collide/interact with a target anode. The technique has improved over the years, with the introduction of high emulsion film, scintillating screens, tube filters, better generators, and grids; however, the principle remains the same(80). All densities along every beam of radiation add up to the total absorption of tube radiation for each pixel, projecting all the

3D data of the object on top of each other as a single image. Thus, much information is lost, or difficult to subtract from the image.

4.2 Magnetic resonance imaging (MRI)

MRI is an old technique described in 1937 by Professor I.I. Rabi in New York. In 1977, the first medical human scan was performed, and since then, MRI has become exceedingly important in the diagnosis and characterization of pathological change. MRI scanners are expensive, technically challenging, and hugely dependent on computer power. The MRI machine consists of a very strong magnet perpendicular to the bore opening, for clinical use often with field strengths of 0.5-3 Tesla (T). The magnetic field interacts with atoms with magnetic properties by using a radio frequency pulse. The body consists of many atoms with magnetic properties, such as 1Hydrogen (H), 13Carbon (C) and 31Phosphor (P); however, the abundance of 1H in fat and water makes it the only atom suitable for imaging. Hence, all MRI scans are therefore calculated from the signal of water and/or fat alone. When a body is placed into a magnet, the field will affect all its H protons, and at 1.5 Tesla, around 9 per 2 million (0.00045%) will align in the direction of the main field. This may not seem much, but since there are 0.67×10^{23} protons per ml of water, there are still around 3.0×10^{17} excess protons aligned along the magnetic field per ml; enough to make imaging possible(80). The part of the body that is to be imaged is divided into voxels (volume units) that together will form an image, as the intensity per voxel is measured and projected as pixels. The technician decides on voxel size before the scan is done, to be either small, for high-resolution imaging, or larger for low-resolution imaging. When the body is placed into the centre of the magnet, every voxel will become magnetized, and the size of these individual magnets can be measured, and is displayed as different brightness in the MR image. It is not possible to measure the size of these individual magnets when they are still aligned along the main field, also called the B0 or z direction. In order to measure their size a radio frequency pulse is applied selectively to the voxels that one wants to measure, this slice or volume selection is done with additional magnetic gradients. As soon as the individual magnets are tilted perpendicular to the main field they start to rotate perpendicular to the main field and its size can be measured with a receiver coil. The signal will lose its strength quickly due to magnetic field inhomogeneities and intrinsic T2 mechanisms according to a Free Induction Decay (FID) curve (figure 4.1).

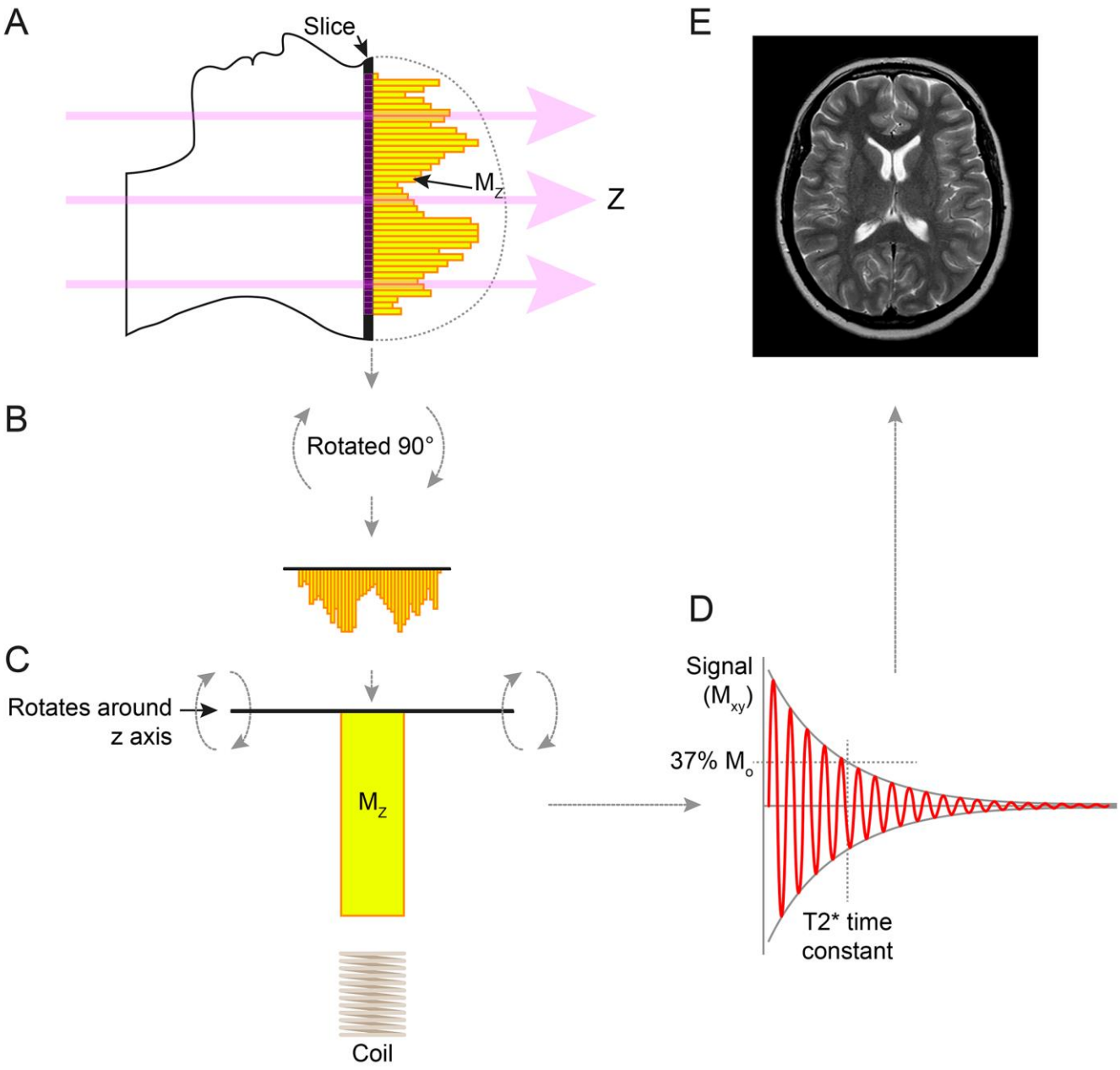

Figure 4.1 A: When the patient is placed in the magnet with field direction Z, every voxel will become magnetized (Mz). The number of voxels within each slice is determined by the "in plane" resolution. B: Before the size of the individual magnets can be measured they are tilted perpendicular to Z into the direction of the coil. C: All the signals from all the voxels comes together by the 90-degree pulse and are measured as one signal called the FID. D: FID signal

that has to be decoded by 2D Fourier transformation to calculate the Mz of the individual voxels. This gives the image, with bright pixels for a large Mz and dark pixels for a small Mz.

This resonance signal is best recorded with a coil that is sensitive, and close to the patient. Movement during the scan is one of the many factors that can degrade the image quality and should be avoided. The resonance signal is relatively weak and disappears quickly, normally in around 30 milliseconds. This signal is called the FID, and is used for gradient echo imaging. The signal strength of the FID decays according to the T2* curve. By using a refocusing pulse such as the 180-degree pulse, one can extend the measurement period substantially by creating the spin echo, thus compensating for all constant field inhomogeneities that contribute to signal decay of the FID (figure 4.2). The strength of the signal measured in the receiver coil will be translated to brightness relative to the other voxel signals in the image, where every measured voxel will be represented as a more or less bright pixel. The values that are thus measured in imaging are not absolute values like the CT Hounsfield scale but intensities relative to each other. This is the reason for the rescaling that occurs in fat suppression and contrast enhanced imaging, amongst others.

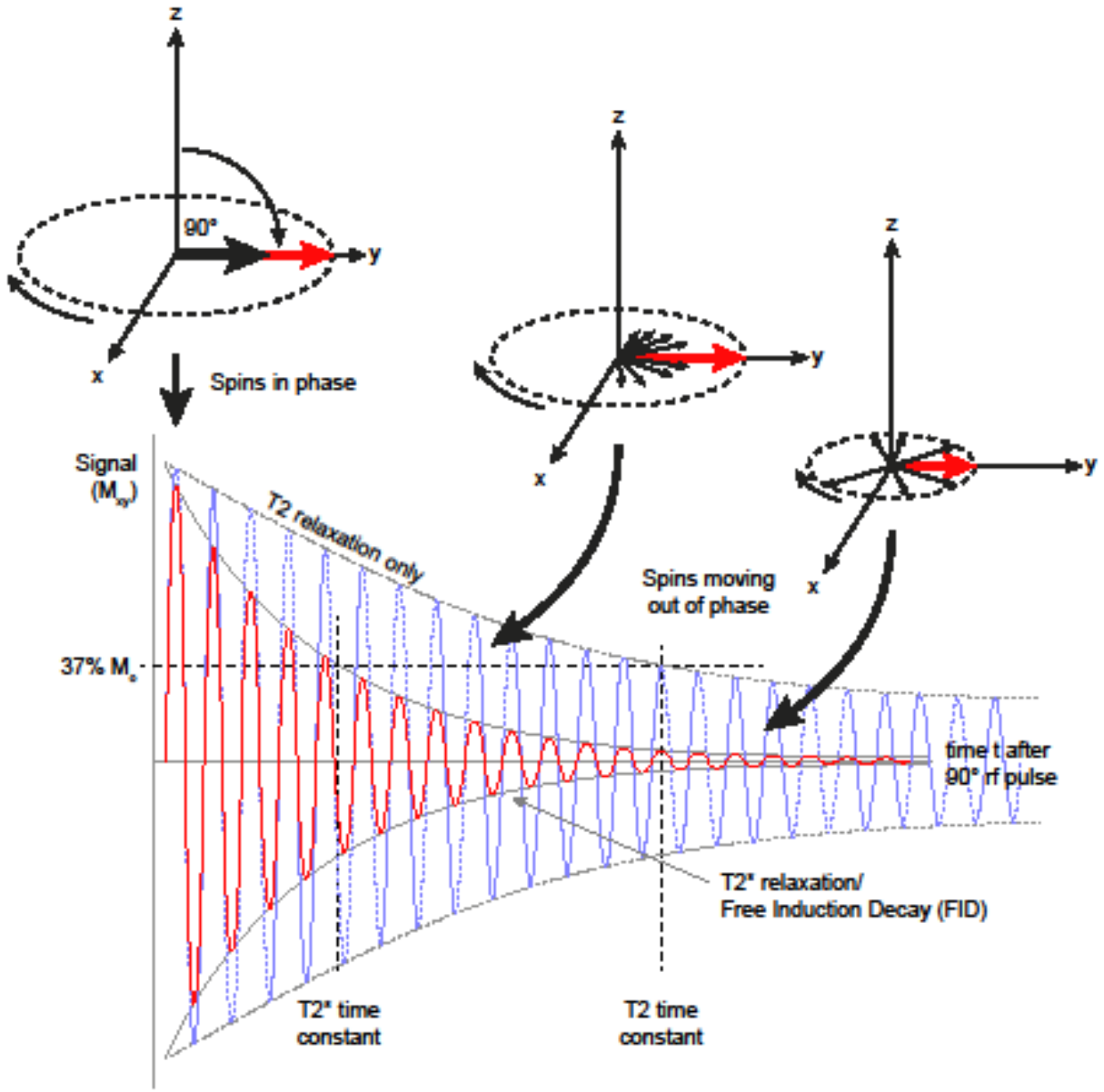

Figure 4.2 Illustration of the decay of the FID (red) due to T2 effects of dephasing of all the individual Mz vectors, and the blue decay illustrating the decay in spin echo where there is more signal for a much longer time, the T2 decay.*

4.2.1 Image weighting

By changing the scan settings, the operator can enhance certain tissue properties such as for instance the T1 values; such a sequence is termed T1 weighted. Other weightings are T2, Proton, and Diffusion weighting. The sequences can be done with or without fat suppression, or fat saturation (figure 4.3).

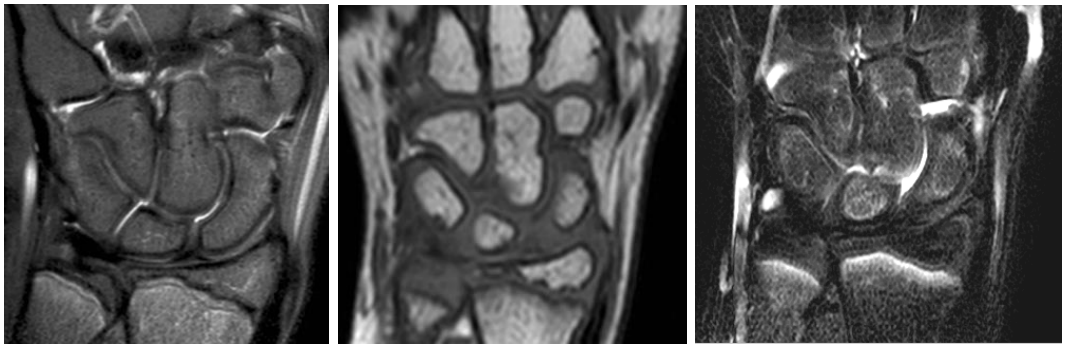

a) b) c)

Figure 4.3 Coronal MR images of the wrist showing commonly used weightings, a) a proton density weighted image with fat saturation b) T1 weighted image and c) T2 weighted image with fat saturation.

Proton Density

Proton density or PD images measure the combined fat and water 1H proton signal per voxel. This signal is equivalent to the number of 1H atoms in the voxel. To achieve this particular weighting one has to wait long enough before every measurement, so that every voxel is fully magnetized, normally 3-5 seconds, before tilting them to the measurement plane or x-y plane. The measurement is performed early in the FID or with short echo times, in order to avoid signal loss due to the natural decay of the signal. A disadvantage of this type of image is the relative low contrast between tissues; an advantage is the relative high signal that allows for high-resolution imaging. This weighting is often used in musculoskeletal imaging in a combination with a fat saturation pre pulse for higher tissue contrast, and higher sensitivity to pathology.

T1

The T1 property of a tissue can be described as the speed of magnetization. When tissue is placed in the strong B0 field it takes some time for it to be fully magnetized and reach its maximum size. Different tissues have different T1 properties; fat has a fast magnetization and reaches maximal value much faster than water. This speed is measured in the T1 value of the tissue; T1 is short for fat and long for water. If we want to demonstrate the T1 properties in the image, we have to choose the imaging parameters accordingly. This means that if we wait for a long time, long enough for every voxel to reach maximum, we would lose the information on speed. If we would tilt the voxel magnets in the x-y plane, directly after the last measurement, then many would not have reached maximum due to long T1 times and that would be shown in the image as T1 contrast. In a T1 image a long T1 time would mean low signal and dark pixels, a short T1 time would give bright pixels. The time between measurements, also called repetition time (TR), needs to be short for T1 weighting to happen, for spin echo imaging around 0.5 seconds (figure 4.4).

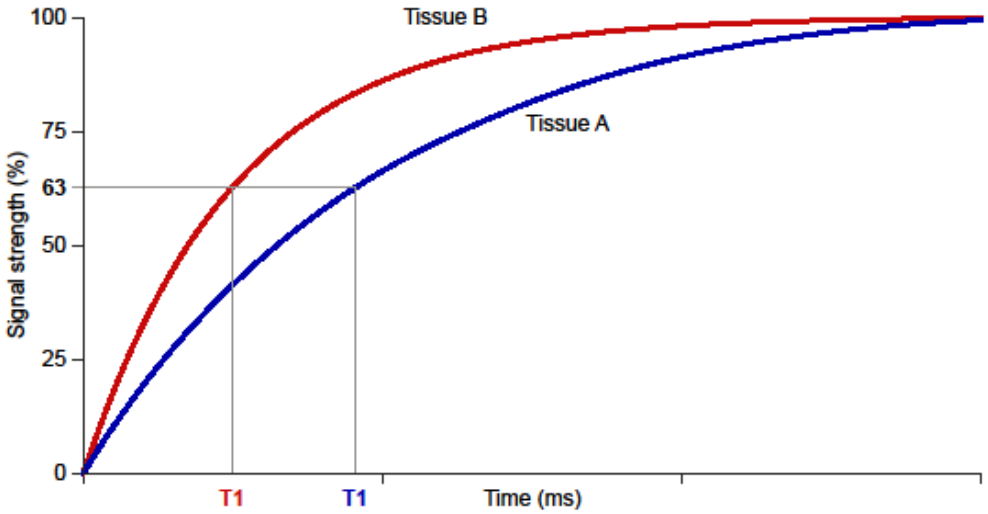

Figure 4.4 T1 curves for two different tissues, tissue A has a longer T1 time (slower rise of magnetization Mz after a 90 degree pulse) than tissue B. When a new 90-degree pulse is given before full magnetization of Tissue A, there will be a difference in signal strength and pixel intensity between the two tissues with tissue A being darker. This is called T1 weighting.

T2

In T2 weighted imaging we look at the speed of signal decay. As soon as the small voxel magnets are tilted to the x-y plane for the resonance signal to be measured, they will lose this signal because of the strong external magnetic field (B0) that forces them to rebuild their magnets in the Z direction. This decay is described as the T2 in spin echo imaging (and T2* in gradient imaging). When a tissue has a long T2 value this means that it takes a long time before the signal disappears from the x-y plane. If we choose to measure directly after the magnets are tilted, we would not measure any T2 properties as the different tissues just had started with their individual decays. For an image to be T2 weighted we must then wait a bit before we measure, this waiting period is the time to echo or TE, it is thus short for little or no T2 weighting and longer for T2 weighting (figure 4.5). In spin echo imaging an echo time of 40 milliseconds (ms) would be short and 120 ms would already be long. The final contrast in the MR image is dependent on a combination of TR and TE; long TR and TE gives T2 weighting, short TR and TE gives T1 weighting, and long TR with short TE gives PD weighting. There are of course other factors that influence contrast in the final image as well, such as saturation or inversion pre pulses, magnetization transfer contrasts, diffusion, magnet inhomogeneity's, movement, B1 distribution, flow, gadolinium contrasts, turbo and echo planar imaging factors.

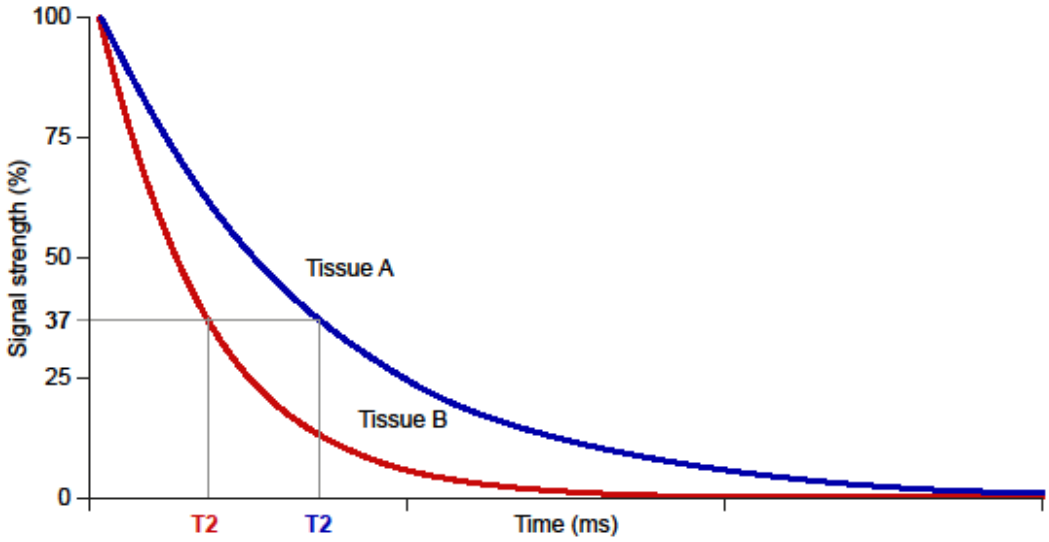

Figure 4.5 Signal decay curves in the perpendicular plane of two tissues, tissue A has a slower decay and will return more signal than tissue B being brighter in the image. This effect gets stronger with longer echo times as the signal is equal, to start with, for both tissues. This is the basis for T2 weighting.

Newer MR imaging sequences

Besides the original T1, T2 and proton weighted sequences there are currently several others on the market, all with its own properties.

Diffusion weighting is a relative new method that measures the amount of free water movement or Brownian motion of the water molecules, by applying an additional dephasing and rephrasing gradient to a spin echo combined with an echo planar imaging (EPI) sequence. The extracellular fluid moves more restricted when there is a high cell density like in the inflamed synovium and returns more signal than the normal synovium in these inherent T2 weighted sequences. Recently, the diffusion weighted Turbo Spin Echo (TSE) sequence was introduced to overcome the T2* effect of bone and this sequence can therefore probably be of use for measuring diffusion coefficients within the bone.

5 Research context, aims, design and methods

5.1 Research context for this thesis

In a collaborative study between four large paediatric centres (London, Paris, Rome and Genoa), the Health-e-Child study was set up with an overall aim to find biomarkers for disease activity in children with JIA. The development of an MRI scoring system for wrist and hip involvement in JIA was among the principal objectives for this study. The resulting method for wrist involvement encompasses four independent imaging parameters of disease activity: the degree of bone marrow oedema-like change and volume of bony erosions in the carpal bones, severity of synovitis at five sites within the wrist (radioulnar, radiocarpal, midcarpal, 1st carpo-metacarpal joint and 2nd-5th carpo-metacarpal joints) and the severity of tenosynovitis involving the flexor compartment and three extensor tendon compartments. However, initial findings suggested that some of the features seemed independent of disease activity and severity(1). Moreover, results from the Tromsø-wrist-cohort showed that several of these features actually appear in healthy children and as such do not necessarily represent disease. It is therefore crucial for future diagnostics, both with regard to JIA and to other conditions, to characterize the appearances of normal maturation of the wrist over time. Leading paediatric musculoskeletal radiologists and clinical rheumatologists are now involved in devising new scoring systems for hip- and wrist involvement of JIA.

5.2 Aims of the study, design and sample size

The overall aim of this study was to investigate the appearances of the wrist in healthy children by age, as assessed on MRI and radiography. More specifically, we aimed to (papers I-IV):

1. examine the prevalence of bony depressions, joint fluid pockets and bone marrow-oedema-like change as assessed on MRI
2. compare the numbers of bony depressions as assessed on MRI and radiography
3. examine the development of bony depressions over time
4. examine the prevalence of joint fluid, bone marrow oedema-like changes and ganglion cysts over time

A cross-sectional approach was used to answer research questions 1-2 above, while research questions 3-4 were addressed through a follow-up of the initial cohort, i.e. a longitudinal cohort study.

Sample size

Based on existing literature on MRI of the foot (76, 81) and on previous experience from imaging children, we inferred that bony depressions, bone marrow-like change, and joint fluid on wrist MRI might be seen in healthy children. By using an educated guess that carpal depressions would be seen in at least 10% of healthy children vs. a reference value of 0, a sample size of 95 children would have a 90% chance of detecting a significant difference at the 5% level. Similar, a sample size of 42 would be required to detect a difference of 20% (82-84).

5.3 Subjects, inclusion and exclusion criteria

The Tromsø cohort consists of 89 healthy children aged 5-15 years from the city of Tromsø, who were all recruited during the period March to October 2009. The invitation was announced on clipboards and via e-mail at the University Hospital North Norway (UNN) and at primary schools in Tromsø. The cohort was recruited using stratified (age and sex) random sampling to provide a balanced dataset. Exclusion criteria were: contraindications to MRI, chronic disease, medication, and recent trauma, i.e. within the past 4 weeks. One of the examinations was incorrectly filed in the PACS system at UNN, leaving 88 examinations (in 88 children) for analysis (figure 5.1). Only one child was 5 years of age (5 years and 9 months), and this was rounded up to 6 years for analysis.

The cohort was re-approached by postal letter and invited for a follow up during autumn 2013. 74 children accepted the invitation and were subsequently scanned using the same protocol except for an additional sequence that was added for cartilage visualization.

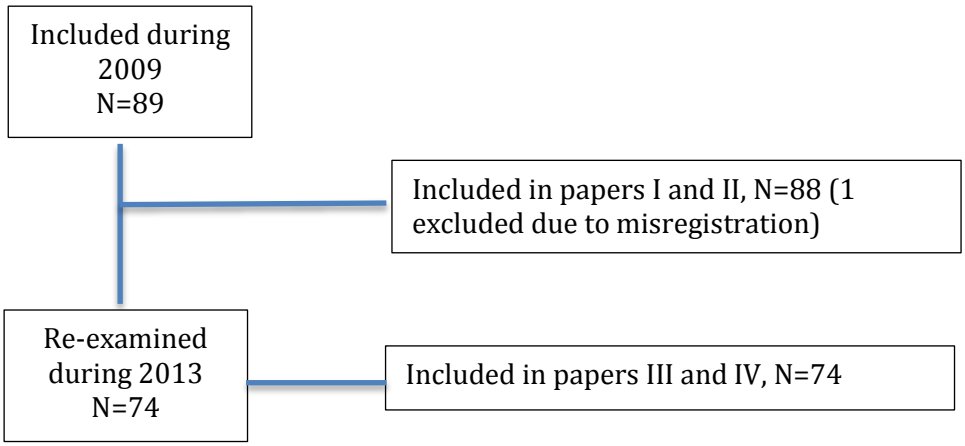

Figure 5.1 Flowchart of participants in the Tromsø cohort.

5.4 Methods and analysis

All children found eligible for the study had an MRI examination and a radiograph of the left wrist taken on the same day, at the Department of Radiology, UNN. The baseline examinations were performed during 2009 and the follow-ups during 2013.

5.1.1 MRI examination

All imaging was done on a clinical 1.5 Tesla MRI scanner, Philips Medical Systems Best the Netherlands, Intera model release 2.3 with master gradients and a 4-element wrist coil. The repeat imaging was done with the same equipment. All scans were performed with the child in a prone position with the hand off- centre in a neutral position alongside the body. No sedation was used. The following sequences were performed:

T1 weighted imaging

The T1 weighted sequence was performed as a coronal FSE TR 561 TE 6.8 with 3 echoes and NSA 6 with 40 slices in 3 stacks (figure 5.2). Slice thickness was 0.9mm and acquired voxel size was 0.69x0.72x0.90mm, with a reconstructed voxel size of 0.25x0.25x0.90mm. Parallel imaging was used with a reduction factor of 1.6, giving a scan time of 4 minutes 11 seconds.

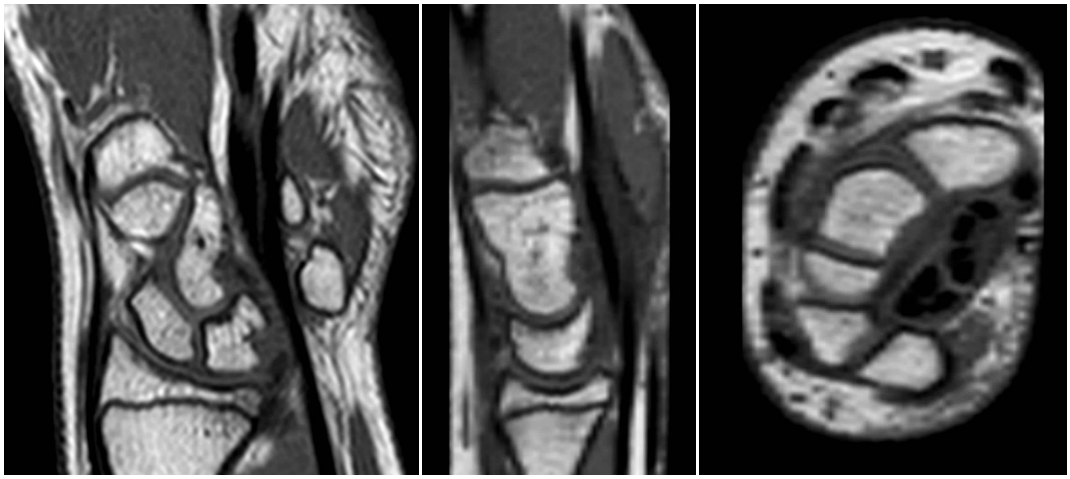

a) b) c)

Figure 5.2 Coronal T1 weighted image (a) and sagittal (b) and axial (c) reconstructions.

T2 weighted fat saturated imaging

The T2 weighted, FSE sequence was performed in the coronal plane, using the following parameters: TR 3165, TE 70, 10 echoes, fat suppression using SPAIR (Spectral Selection Attenuated Inversion Recovery) NSA was 4 with 14 2.5mm slices giving an acquired voxel size of 0.31x0.40x2.50mm and a reconstructed voxel size of 0.15x0.15x2.50mm. Scan time was 3 minutes and 56 seconds (figure 5.3).

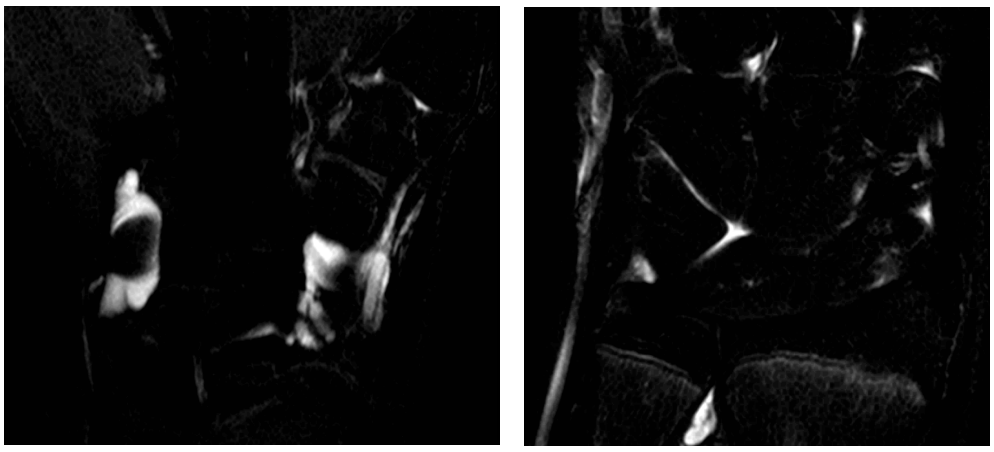

a) b)

Figure 5.3 T2 weighted, coronal images with joint fluid pockets (a, b).

Cartilage imaging

The cartilage sequence was a coronal 3D WATSc (WATer Selective cartilage) sequence with 60x0.75mm slices and an acquired voxel size of 0.38x0.38x1.5mm. Scan time was 4 minutes and 7 seconds. Reconstructions into 0.75 mm slices were performed (figure 5.4).

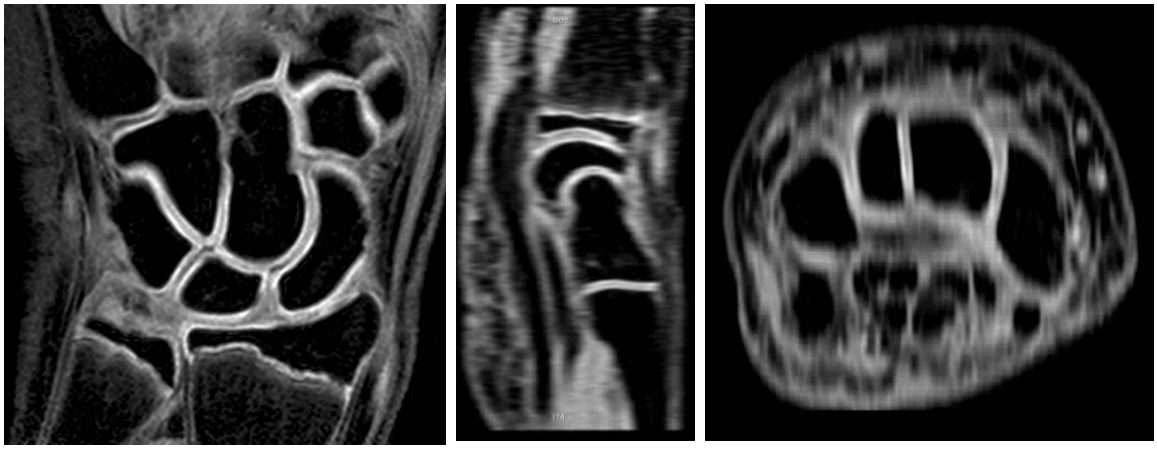

a) b) c)

Figure 5.4 Cartilage specific images, a) coronal, b) sagittal reconstruction and c) axial reconstruction. The cartilage appears bright and the joint fluid is dark.

5.1.2 Radiography

Radiographs of the left hand were performed on a Triathion Direct digital system (DR)(Decothron AS Skedsmo, Norway) using 50 KVp and 2.0 mAs as standardized setting. The Varian x-ray tube had a permanent filtration of 0.7 Aluminium (Al). The radiation dose was around 11.3 mGy cm2. The bone age was obtained by using the automated computer program BoneXpert (Visiana Aps, Holte, Danmark)(85).

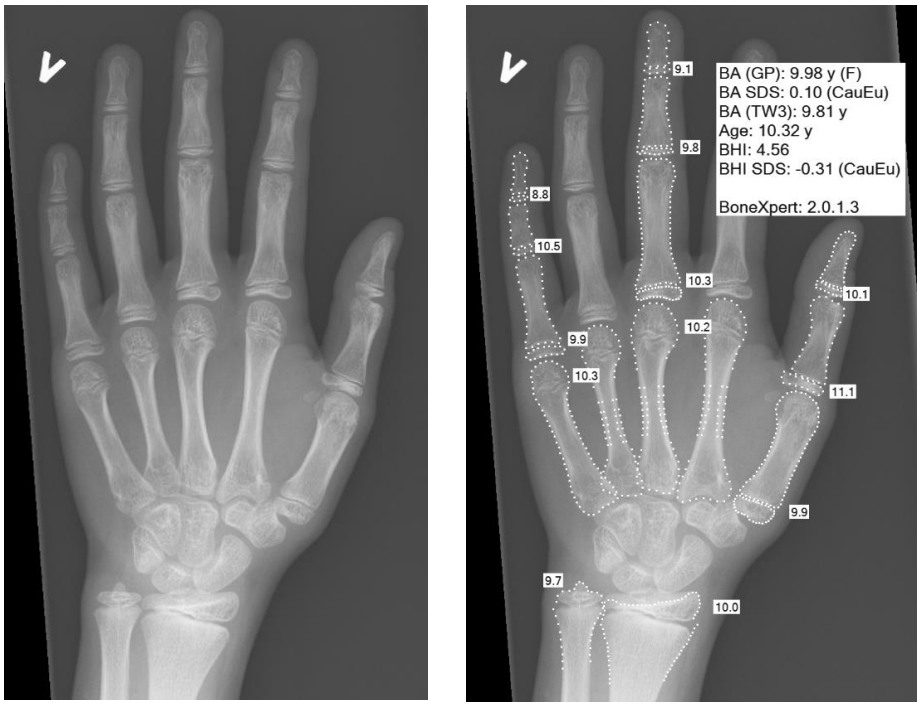

Figure 5.5 Radiograph of the left hand in a 11-year-old girl, using an automated bone-age analysis tool (BoneXpert).

5.5 Image analysis

All the MRI scans and radiographs were analysed in consensus by two radiologists with a special interest in musculoskeletal radiology using high-resolution screens. K. Rosendahl, together with either LS. Ording or D. Avenarius, performed the image reading sessions. For paper 4, all three investigators scored in consensus. All reading sessions were performed masked to the results of previous readings. Again, bone marrow oedema-like change was defined as a lesion within the trabecular bone, with ill-defined margins and signal characteristics consistent with increased water content, returning high signal on T2 weighted and low signal on T1 weighted images. The presence and distribution of bone marrow oedema-like change was noted for each of the following bones: distal radius and ulna, all carpal bones except for the pisiform and the basis (proximal 1cm) of the 1st to the 5th metacarpal bones. On a second assessment, the extension of change was scored subjectively as 0 to 3 (0=no change, 1=1-33% of the volume involved, 2=34=66% and 3=67-100% of the volume involved). This 4-category system of scoring was chosen for its reliability(86). Presence and volume of joint fluid was assessed based on the T2 weighted

images, and scored as 0 (none), mild (maximal thickness < 2mm) or moderate (maximal thickness ≥2mm). Bony depressions were defined as cortical depressions, focal or tubular, other than the normal vascular channels seen on the coronal T1 weighted images, and visible in at least one of the other reconstructed planes (axial and/or sagittal). In addition, we registered whether or not the depression was covered by cartilage (no-yes) on the cartilage sensitive sequence using the reconstructed planes for confirmation.

The radiographs were also evaluated for bony depressions, defined as a focal bone concavity or a well-defined lytic lesion within the bone. In addition it was also noted if the lesion had a sclerotic rim. Depressions identified on MRI and radiographs were marked on separate templates, and the scoring templates were compared side by side in an additional session. The degree of bony maturation, or bone age, was assessed from the radiographs by using the automated computer program BoneXpert (Visiana Aps, Holte, Danmark(85) (figure 5.5).

5.1.3 Data collection and storage

Data (textual and numerical) were registered and stored in a common database (SPSS), while images were stored in the PACS system at UNN according to established clinical routines. All other papers like consensus forms and sheets with biometrical data are stored in a locked office at the department of radiology, UNN.

5.1.4 Statistical analysis

Statistical analysis paper 1:
A one-way between-group analysis of variance (ANOVA) was performed with age as the independent variable and number of bony depressions as the dependent variable to detect the impact of age on the number of bony depressions, with post hoc tests to determine where the difference among the age groups occurred. Chi square tests were used to examine possible associations between age and the proportion of children with bone marrow changes (dichotomized), and visible joint fluid (linear by linear associations with exact tests as appropriate). Based on total scores for bony depressions (sub grouped as 0-2, where 0=<5 depressions, 1=5-10 depressions and 2=10 or more), bone marrow change

and joint fluid, chi square tests were used to examine possible associations between sex, sports club membership, time of the year for the examination (snowy season or not) and MRI findings.

Statistical analysis paper 2:

Also here the one-way between-group analysis of variance (independent variable age, dependent variable; number of bony depressions) was conducted to explore the impact of age on the number of bony depressions. Findings were divided into four groups, both according to chronological age group of the children and to bone age as assessed by the BoneXpert program (85). Chi square tests (Pearson Chi square, exact significance, 2-sided) were used to examine possible associations between bony depressions and handedness, sports-club membership and sex. One-way between-group analysis of variance was performed to compare the number of depressions by age group (both bone age and chronological age).

Statistical analysis paper 3:

The children were grouped according to chronological age, using the same grouping used in 2009, for direct comparison. A chi-squared test was used to examine possible associations between sex and number of bony depressions. We performed a one-way between-group analysis of variance (independent variable age, dependent variable number of bony depressions) to examine the impact of age on the number of bony depressions and on the rates of depressions covered with cartilage (dichotomized).

Statistical analysis paper 4:

In this follow-up study we divided the children into the same four groups that were used in the initial study. Chi squared tests were used to examine possible associations between age and the proportion of children with bone marrow changes (dichotomized) and visible joint fluid (linear by linear associations with exact tests as appropriate). Based on total scores for bone marrow oedema like change and joint fluid, Chi squared tests were used to examine possible associations between sex, number of training sessions per week and MRI-findings.

The use of arbitrary age groups could have been omitted by using a regression analysis, using the exact age and gender as independent variables, and number of depressions, amount of joint fluid, and amount of bone marrow oedema-like change as dependant. An advantage would have been that no separate analysis for gender differences would have been needed. However, the models and the information are the same, and the results did not differ from the preliminary regression analysis that was performed. The reason we kept the age groups throughout was the idea of creating an atlas with MRI appearances by age; hence 4 groups appeared reasonable for practical purposes.

The analysis were performed using SPSS Versions 17/23; $p<0.05$ was considered statistically significant.

5.1.5 Ethical approvals

Informed consent was given by children ≥16 years of age, and by their parents if under the age of 16. Younger children were informed of the study by their parents. The Tromsø cohort-study was approved in 2009 by the Regional Ethics Committee, Northern Norway (REK number: 5.2009.295), and again in 2013 (reference number 2013/385/REK North)

6 Main Results

Paper 1

The paediatric wrist revisited: redefining MR findings in healthy children.
Müller LS, Avenarius D, Damasio B, Eldevik OP, Malattia C, Lambot-Juhan K, Tanturri L, Owens CM, Rosendahl K.

This study was based on the initial consultation of the healthy cohort including 89 children aged 5-15 years, examined during 2009. The coronal T1 weighted MRI scans of 88 (44 males) healthy volunteers were examined for bony depressions resembling bone erosions

according to the OMERACT criteria of adult patients with rheumatoid arthritis, e.g. a sharply delineated bone lesion with correct juxta-articular localization and typical signal characteristics, with a cortical breach visible in two planes. For this reason the scans were reconstructed in axial and sagittal planes. The T2 weighted fat suppressed scan was analysed for joint fluid pockets and bone marrow oedema-like change. Four T1 weighted scans and four T2 weighted scans were of inferior quality leaving 84 scans for analysis.

The total number of bony depressions increased significantly across four age groups (5-7 years, 8-9 years, 10-11 years and 12-15 years). A similar increase was seen for individual bones apart from the hamate. There were no differences according to sex or sporting activity. All children had visible joint fluid in at least one compartment, and no associations were seen between the presence of fluid and age group except for the radius /scaphoid and capitate-scaphoid joints and a recess lateral to the hamate. There were no differences in fluid according to sex except for the second carpometacarpal joint, which had a moderate volume of joint fluid in seven boys but only in two girls (p=0.040). No associations were found between the presence of joint fluid and sporting activities. Forty-five (23 boys) of 84 children (58.6%) showed high signal on the T2 weighted images with corresponding low signal on the T1 weighted images, indicative of bone marrow oedema in at least one of the bones that were assessed, including the distal radius. No associations were seen between the presence of bone marrow oedema-like change and sex, sporting activity, or season.

Paper 2

The paediatric wrist revisited - findings of bony depressions in healthy children on radiographs compared to MRI.

Avenarius DM, Ording Müller LS, Eldevik P, Owens CM, Rosendahl K.

This study addresses the occurrence of bony depressions amongst the healthy children examined during 2009, comparing MRI and radiography. 88 children were included of who four had inferior T1 weighted scans and one had no radiograph, leaving 87(43 males) radiographs for analysis and 84 (43 males) MRI scans.

Radiographically, a total of 75 bony depressions in 50 (23 males) (57.4%) out of the 87 children were identified. 51 were seen in the capitate, 10 in the hamate, 4 in the scaphoid, 3 in the lunate, 3 in the triquetrum, 3 in the trapezoid, and 1 in the trapezium. Thirty-three (44.0%) of the depressions had a sclerotic rim. There was no statistically significant difference in the total number of radiographically detected depressions across age groups, and no difference according to age for any of the carpal bones. Moreover, no difference in the total number of depressions was seen according to handedness (p=0.840, Pearson Chi square test) or sport club membership (p=0.333, Pearson Chi square test).

Of the 75 depressions seen radiographically, 64 (85.3%) were identified on MRI, 11 were seen on radiographs alone, most commonly in the hamate. Concordant findings were most often seen in the capitate where 50 of the 51 (98.0%) radiographically detected depressions also were found on the MRI, while this was true for only 6 out of 11 (54.5%) depressions seen within the hamate.

Bony depressions were also seen in the base of the metacarpal bones, 65 in 55 children, with no difference across age groups and no association with sex, handedness, or sports club membership. 81 depressions were seen on MRI in 53 children and here sports club members had significantly more depressions then non-members (p=0.013 Pearson Chi square test), but no associations were seen between handedness and sex, and no differences were seen across the age groups. 53 of the depressions on the proximal metacarpal bones were seen on both modalities, 22 were seen on MRI alone, and 6 were seen on radiographs only. Depressions were not seen on the articular surface of the metacarpal bones, except for the dorsal aspect of the second metacarpal bone where an indentation was seen in 51.7% of the children.

Paper 3

Erosion or normal variant? 4-year MRI follow-up of the wrists in healthy children.
Avenarius DF, Ording Müller LS, Rosendahl K.

This study addresses the presence and development of bony depressions, and the usefulness of an additional cartilage sequence.

The initial Tromsø-Wrist-Cohort included 89 healthy children aged 6-15 years. After an interval of 4 years, the cohort was approached a second time by postal mail, and invited for a follow-up MRI and radiograph of the left wrist. 74 (83.1%) children, now aged 10-19 years, accepted the invitation. On arrival to the Radiology department, all children were asked whether or not they had sustained recent injuries to the left wrist, e.g. within the last 2-3 weeks, and asked whether or not they did organized sports/training, and if yes, type and number of training sessions per week. None of the children had sustained recent injury to the wrist, and all had remained healthy with no signs of inflammatory joint disease. All 74 re-examinations held acceptable technical quality, as opposed to 84 (44 males) on the initial MRI; leaving 71 children (33 males) with two acceptable MRI scans for longitudinal analysis. All 74 follow-up scans were used for assessment of cartilage. Eight of the children/adolescents (4 males) were left-handed. The number of organized training sessions in addition to the normal school gymnastics varied from none to 10 weekly (mean 3.4, SD 2.1). No differences in the occurrence of carpal depressions were found between males and females, and the data were therefore pooled for further analysis.

The total number of carpal depressions increased over time with a total mean of 7.7 (range 0–15) in 2009 vs. 13.6 (range 5–23) in 2013. Their location was unchanged in 370 out of 487 (75.9%) carpal sites and in 91 out of 117 (77.8%) metacarpal sites. Twenty-six of 117 (22.2%) metacarpal depressions and 117 of 370 (31.6%) carpal depressions had disappeared.

In total, 426 of the 1,087 (39.2%) bony depressions were covered by cartilage as assessed on the water-selective-cartilage sequence, with a decreasing percentage by age group ($p = 0.001$). Of the 661 bony depressions where cartilage-coverage could not be seen, 177 (26.8%) were located at the insertion of the inter-metacarpal ligaments, 127 (19.2%) at the insertion of the capitate–hamate ligament, 91 (13.7%) at the insertion of the radio–ulnar collateral ligaments, 58 (8.7%) between the capitate and trapezoid bone, and 56 (8.5%) at the volar and dorsal attachments of radial and ulnar carpal ligaments. The remaining 152 depressions were located in other juxta-articular areas.

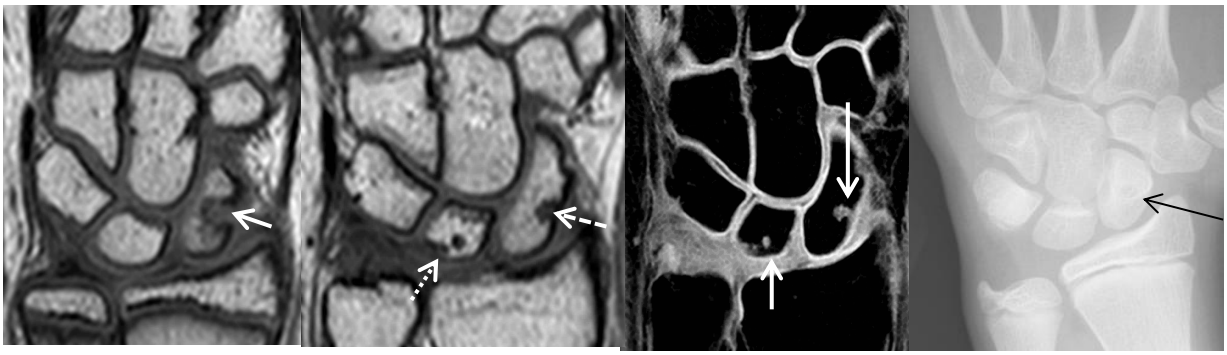

a) b) c) d)

Figure 6.1 a) Coronal T1 weighted turbo spin-echo MR image in a 13-year-old boy shows a large bony depression in the scaphoid bone (arrow), b) at 4-year follow-up the depression is still seen but is less pronounced (dashed arrow). New bony depressions are seen on the surface of the lunate (dotted arrow), c) the cartilage sequence shows that both old and new depressions are covered with cartilage (arrows) and d) radiograph of the same 13-year-old boy shows the scaphoid depression with a sclerotic rim (arrow).

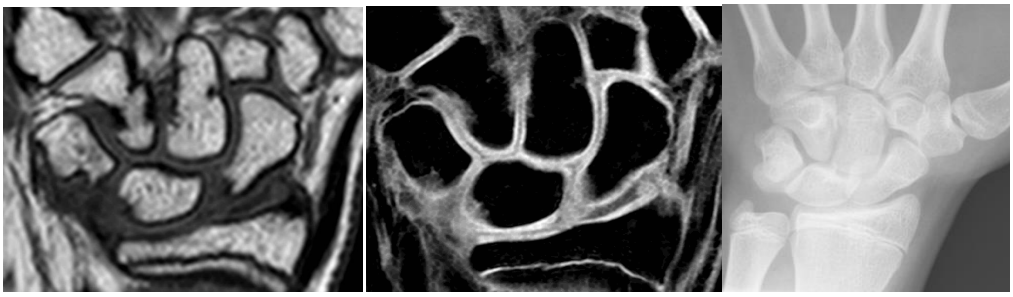

a) b) c)

Figure 6.2 a) Coronal T1 weighted turbo spin-echo MRI in a 16-year-old boy showing several bony depressions in most bones, b) the cartilage sequence shows that all carpal depressions are covered by cartilage, c) none of the bony depressions are visible on the radiograph.

Paper 4

Joint fluid, bone marrow oedema like changes and ganglion cysts in the paediatric wrist; features that may mimic pathology. Follow-up of a healthy cohort.

Avenarius DF, Ording Müller LS, Rosendahl K.

74 (35 males) of the original 89 (45 males) healthy volunteers (83.2%) were included in the follow-up at an interval of 3.7 to 4.8 years (mean 4.2 years, SD 0.2 years). None of the children had sustained recent injury to the wrist, and all had remained healthy. All 74 re-examinations held acceptable technical quality, as opposed to 72 (35 males) on the initial MRI, thus leaving 72 children (35 males) with two acceptable MRI scans for longitudinal analysis. Eight of the children/adolescents (4 males) were left-handed. The number of organized training sessions in addition to the normal school gymnastics varied from none to 10 weekly (mean 3.4, SD 2.1). No statistically significant differences in the occurrence of joint fluid, bone marrow oedema-like change, and ganglion cysts were found between males and females, and the data were therefore pooled for further analysis.

Bone marrow oedema-like change

Bone marrow oedema-like change was seen in at least one bone in 29/74 (39.2%) of the wrists as compared to 35/72 (48.6%) in 2009 (p=0.153). The location differed from the initial examination in all the observed cases. In 15 out of 74 (20.3%) wrists bone marrow oedema-like change was seen in one of the carpal- or proximal metacarpal bones, and in 14 (18.9%) wrists, involvement of more than one bone or of more than 33% of one bone was found. There were no differences in the occurrence of bone marrow change according to age group (p=0.568).
Bone marrow oedema-like change was seen in varying degrees, affecting only a small proportion of a bone, a whole bone or several bones. It was most often seen in the scaphoid or in the capitate. The proportion of wrists with at least one bone involved was higher for the youngest age group. At the initial examination, bone marrow oedema-like change was most frequently seen within the capitate and hamate as opposed to the capitate and scaphoid at follow-up.

The highest total bone oedema-like score in both 2009 and 2013, e.g. more than two bones involved or 66% or more of one bone, was found amongst 9 -16-year-old children only, while lower scores were more evenly distributed across age. In seven cases, bone marrow oedema-like change was present at both sides of a joint. In 13 children and in 20 locations

the changes were adjacent to a bony depression. There was no statistically significant relationship between the number of weekly training sessions and the occurrence of bone marrow oedema-like change (p= 0.80).

Joint fluid

All 74 subjects had at least one pocket of fluid measuring 1-2 mm while 37 (50.0%) of the subjects had at least one fluid pocket ≥ 2mm. Fluid pockets of ≥ 2 mm were found at all locations, and most commonly around the pisiform bone in the pisotriquetral joint (39.2%) and in the intra-carpal joint (16.2%). Opposite, it was rarely seen in the radiocarpal (2.7%), the carpometacarpal 1 (1.3%), the carpometacarpal 2-4 (4.0%), or in the radioulnar joint (1.3%). No association was seen between age and the presence of joint fluid for any of the locations investigated.
The proportion of children with at least one fluid pocket ≥ 2mm did not change significantly during the 4-year period; 44/74 (59.5%) vs. 35/74 (47.3% (p=0.348). The location was unchanged in 23 of 49 (46.9%) joints.

Ganglion cysts

In 18 (9 male) individuals (24.3%), at least one ganglion cyst was seen, all of which were asymptomatic. The youngest child with a ganglion cyst on the first examination was 5 years and 6 months old. A maximum of 3 ganglion cysts were seen in one individual, with the larger measuring 13 mm. Of the 24 ganglion cysts seen at follow-up, 13 were also identified on the initial scan whilst 11 were new. Six ganglion cysts present on the initial scan were not identified at follow-up. 14 (58.3%) of the ganglion cysts were localized on the palmar side. Nine (37.5%) of the cysts were located around the radio carpal joint. One of the ganglion cysts was located in the proximity of bone marrow oedema-like change.

7 General discussion

7.1 Study design

In general, a study can be either experimental or observational. There are three main types of observational studies, namely the cohort study (also called longitudinal or follow-up study), the crossectional and the case-control study. The three types represent different approaches of examining the occurrence of health-related issues such as disease and risk factors within a given time period and population. The current thesis includes *crossectional studies* reporting MRI-based findings of the wrist in healthy children (paper 1) and a comparison of MRI and radiography in assessing bony depressions (paper 2). Moreover, a *follow-up study* was performed to examine the MRI-appearances over time (papers 3 and 4). To obtain a balanced dataset including similar proportions of each sex and all ages between 6 and 15 years, stratified sampling was performed. Stratification is the process of dividing members of the population into homogeneous subgroups before sampling, to secure a *representative sample.*

The aim of all quantitative sampling approaches is to draw a *representative sample* from the population, allowing for *generalization of the results*. One approach is to use random sampling, i.e. that all members of the population have an equal chance of selection. In the present study, the sample was invited / selected via notes on clipboards or e-mails at the University Hospital North Norway or at primary schools in Tromsø. Thus, most of the respondents had at least one caregiver working at the hospital, which may have led to underrepresentation of other socio-economic groups and therefore have biased the results *(response bias). Bias* can be defined as systematic, non-random deviation of a study's results from its true value, and can arise from incorrect subject selection or incorrect information, leading to incorrect associations. In the present study, the rates of left-handedness and children participating in sports were comparable with rates found in the general population(87). Moreover, all children were Caucasians. Thus, all in all we consider the sample to be representative for the general population aged 6-15 years.

The lower age limit was set at 6 years since children this age upwards usually manage to undergo a MRI without sedation. Another factor was that some of the respondents also took part in another study on body MR Diffusion weighted imaging of the pelvis and the lumbosacral spine.

In general, the *size of the sample* is determined by the optimal number needed to enable valid inferences to be made about the population. The larger the sample size, the smaller the chance of a random sampling error, however, since the sampling error is inversely proportional to the square root of the sample size, there is usually little to be gained from studying very large samples. The optimal sample size also depends on the rarity of the features under investigation. One would anticipate that MRI-findings suggestive of disease were non-existent in healthy children. However, based on a few papers and on previous experience, we inferred that at least 10% of healthy children would have MRI- and radiographic features similar to that seen in different pathologies. That number turned out to be higher, hence increasing the robustness of the study.

7.2 Radiographs and MRI protocols

The radiograph of the hand was performed using a digitized XR system according to a standard protocol, with a PA view of the hand. The radiation dose was around 11.3 mGy cm2, corresponding to around 5 days of normal background radiation. This dose was considered negligible and without any clinical relevance.

A T1 weighted sequence is a robust method for visualizing wrist anatomy. It provides good contrast between bone marrow and soft tissues and the bony cortex is well seen despite subtle chemical shift artefacts. A high-resolution sequence was used to enable good reconstructions in other planes, and a TSE technique was preferred over gradient imaging for better delineation of structures, and reduction of artefacts as compared to the frequently used 3D gradient sequences. The sequence was divided into 3 stacks to further diminish the effect of movement on the images. Other sequences, like PD seen in figure 7.1a, can give the same anatomical details with additional cartilage visualization, but we were unable to make the slices thin enough within a reasonable scan time. A T1 weighted sequence is often an essential part of the wrist scan in clinical practice, as it is used before and after intravenous contrast administration. It was therefore preferred over other weightings. An additional argument in favour of the T1 weighting was the good experiences from an already examined cohort of children with JIA (Health-e-Child study).

A T2 weighted fat suppressed sequence, either STIR or T2 weighted Fat saturated by selective pre-pulse, is necessary to visualize bone marrow oedema and can be used for visualization of fluid as well. We chose the T2 weighted sequence as it in general has a better signal to noise and gives images with a higher resolution than the STIR. The images appear rather dark as all the subcutaneous fat and bone marrow fat is suppressed and the Magnetization Transfer Contrast effect turns the remaining water-containing tissues rather dark as well. The slice thickness was increased because of the inhered low signal and reconstructions in other planes were not possible.

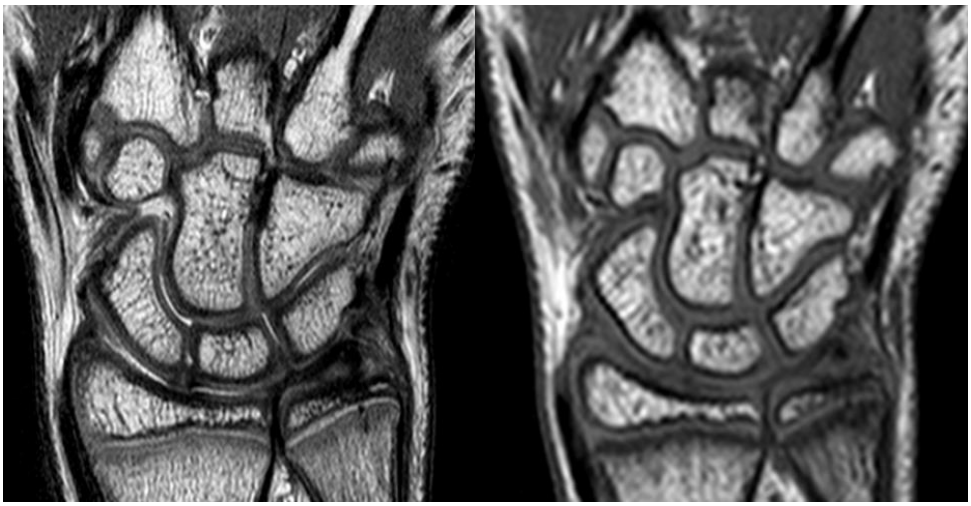

a b

Figure 7.1 Example of a proton weighted image (a) with high resolution and good contrast between joint fluid and cartilage, and its corresponding T1 weighted image (b) with much less tissue contrast.

Several cartilage-imaging methods are used clinically but most of them are developed and tested on adult, articular cartilage. The cartilage in carpal bones has a somewhat different structure of collagen matrix and vessels, and its function differs from that of articular cartilage. We tested a few proton weighted sequences in preparation for the follow up scanning, and found that these had the right contrasts and quality in the coronal plane (figure 7.1a); but the reconstructions were of suboptimal quality due to the slice thickness. Sequences with dark cartilage and bright joint fluid like the T2 weighted FSE

type series can be used to indirectly visualize cartilage, but it would be more difficult to see if bony depressions that are also dark would be covered. In the end we used a relative common WATSc sequence and deliberately did not change the factory settings, making it easier for others to reproduce the findings. The fat in the WATSc sequence returns no signal because of the water selective excitation and the fluid is dark because of spoiling of residual signal. The sequence is a coronal volumetric steady-state spoiled gradient echo with thin slices that can be reconstructed in other imaging planes. The cartilage was to be compared to the T1 weighted images and reconstructions and the WATSc sequence gave comparable reconstructions.

The MRI machine used for this project was a clinical 1.5 Tesla whole body scanner with a four channel dedicated wrist coil. The coil was an adult coil that had to be adjusted with soft materials for use on children. Currently, higher field strength 3 Tesla MRI units and coils with more and improved coil-elements for better signal detection are preferred for MSK imaging. This equipment gives images with higher resolution and/or shorter scan times.

7.3 Reproducibility of the findings

The accuracy of MRI in the assessment of carpal bone erosion/destruction and bone marrow oedema-like change has previously been thoroughly addressed by our research group (86, 88). A scoring system of five categories based on bone volume loss resulted in moderate to good inter-observer agreement for the majority of the carpal bones assessed, while the intra-reader agreement was somewhat better, with simple kappa values between 0.5 and 0.8(88). Likewise, the intra-observer agreement for bone marrow oedema-like change in a study of 76 children with JIA was moderate to excellent, while the inter-observer agreement was moderate to good (86). The kappa coefficient measures pairwise agreement between a set of readers making category judgments, correcting for expected chance agreement. One of the disadvantages of using the kappa coefficient is that the value depends upon the proportion of subjects (prevalence) of each category and it does not distinguish among sources of disagreement.

Experiences from the abovementioned repeatability exercises were shared and discussed, and criteria for the different grading and scores used in the present studies were agreed on and piloted before the scoring took place. All bony depressions were confirmed in at least two planes. A 4-category system, similar to that used in the abovementioned study, was used for the assessment of bone marrow oedema-like change (86).

Scoring of the images was done by two or three radiologists in consensus, and although this method has been criticized for introducing potential bias of semi consensus and neglecting the individual variability within scoring systems, it is still widely used(89). Notably, a recent study provided empirical support for the principle that an additional reader can improve the reproducibility of MRI interpretations compared to one expert alone. Moreover, even a moderately experienced second reader improved the reliability compared to a single expert reader(90).

7.4 Ethical considerations

Some diseases are child-specific and several diseases have different courses in adults and children. Different presentation and symptoms according to age have, in some instances, been misinterpreted as representing two different diseases rather than different expressions of the same disease. Therefore research has to be performed on children, especially in the case of child-specific diseases(91).

There were three main ethical issues related to the Tromsø project: First, incidental MRI findings were seen in one of the presumed healthy subjects, who were subsequently referred to the orthopaedic outpatient clinic. The findings did not turn out to be of a sinister character, and the child was dealt with in a prompt and safe way. Second, a radiograph of the hand includes a minor radiation dose of 0.03 mSv to the child, however, compared to the natural background radiation of 2-5 mSv per year, the dose is of no clinical significance. Third, data security was handled according to the existing regulations. All aspects of the project have been approved by the Regional Committee for Medical Research Ethics (REC-North number: 5.2009.295 for the 2009 examination and REK number 2013/385 for the 2013 follow-up). Since this research was performed on healthy individuals special care

was given as not to cause any distress to our volunteers. All participants received age adjusted written information (see appendix), were shown the MRI unit in advance, and were informed that they could abort their participation at any moment. One of the responsible researchers was always present when the scan was performed to check on the participant's wellbeing.

None of the above ethical issues were violating the Norwegian law regulating medical research, 'Helseforskningsloven' §18, stating that in all medical research the disadvantage or risk from participation in a research project must be insignificant, that all participation must be voluntarily recruited (§18b) and that informed consent must be obtained and that the research should be beneficial for the research 'object' itself or for other individuals with similar age-specific illness or disease (§18c).

7.5 Imaging findings

7.5.1 Bony depressions

Bony depressions or features that resemble erosions according to the OMERACT-criteria were frequently seen in the carpal and metacarpal bones in our healthy subjects. The presence of bony depressions in an adult population has previously been reported for a Finnish cohort, though with fewer depressions per subject(92). We found an increase in the number of depressions with age. This is not surprising as the bones mature from a tiny round ossification centre to a complex form with multiple angulations, articular spaces and with many connecting ligaments. The analysis of the radiographs revealed significant fewer depressions, which in part may be explained by the fact that the MRI examinations contained around 40 images as compared to one radiograph. Some of the radiographic findings could not be seen on the MR images and it is possible that some of these findings represent over projections of the trabecular bone network. Some of the depressions from the first examination were not recognised at follow up, and it seemed that the amount of depressions peeked for some of the bones just before maturity was reached. The increase was seen particularly at the bases of the metacarpal bones and in the triquetrum, scaphoid, capitate and lunate bones, all representing areas of significant growth during the study period of four years. This can be explained by the irregularities of osteochondral ossification occurring during normal maturation but that disappears at skeletal maturity. Ligament attachment sites were often seen as irregular pits and thus scored as

depressions; these ligament insertion sites are constant and increasingly visible over time, in part explaining the trend towards more depressions with age. The irregularities of osteochondral ossification could sometimes be rather pronounced and would certainly be reported as disease in a clinical setting (see figure 6.1 and 6.2). The cartilage in the carpal bones and epiphyses of children is vascularized and the use of gadolinium contrasts would probably not help in the differentiation of these lesions vs. true erosions in a JIA patient.

7.5.2 Cartilage covering

To better visualize and characterize the bony depressions we added a cartilage sequence to the original T1 weighted and T2 weighted fat saturated sequences at follow-up. We assumed that true erosions are not covered with cartilage and that a layer of intact cartilage seen over a bony depression is a marker of normality. This assumption is based on the facts that JIA involves the synovium, and that osteoclast formation is seen adjacent to the synovium, at the surface of the bone(93). Opposite, osteitis, with lymphoid cells and osteoclasts is predictive of later erosions in adults, inferring that erosions can start from the inside, rather than from the outside of the bone(26, 94-96). Regardless of the mechanism, one might assume that cartilage overlying a bone erosion would be damaged.

The amount of cartilage covering different areas of the bone varied significantly in our study. Moreover, the MRI-contrast was sometimes too small to allow for differentiation between cartilage and soft tissues. This was particularly the case for the dorsal and palmar sides of the bones and is probably due to the characteristics of the chosen cartilage sequence. In other locations such as the articular surfaces, the contrast was better. Since these are predilection sites for erosions, we believe that an additional cartilage sequence may be helpful to differentiate between normality and pathology.

Younger children have more and thicker cartilage resulting in more depressions being seen as covered, particularly at the base of the metacarpal bones where coverage was only rarely seen in the three oldest age groups.

7.5.3 Other ways of imaging cartilage

Cartilage can be imaged in many different ways. Sometimes small tweaks to existing sequences may make visualise the cartilage possible, and completely new approaches can even give information about the molecular structure of the cartilage. In traditional imaging it is known that all types of hyaline cartilage will have high signal on proton-weighted images, by increasing the TE on STIR or T2 weighted images one can see a difference; the articular cartilage and growth plate will still have a high signal but the epiphyseal cartilage will have a much lower signal, enabling a differentiation(75). Increasing the TE time will increase this signal difference.

T2 relaxation time mapping is a way of quantifying T2 imaging, the T2 decay is the reason for the different signal intensities on T2 weighted images and the corresponding T2 value can be calculated and displayed on a corresponding image with a colour code making differences in T2 values more conspicuous. The T2 value is dependent on water content and collagen ultrastructure, and damaged areas may show decreased or increased water content and thus variation from normal T2 values(97, 98). This has been used to determine water content in articular cartilage in osteoarthritis as a way of early detection of osteoarthritis. The water content affects the T1 value and the T2 value and these are both positively correlated and can be depicted as a colour map over an anatomic image(99).

We preferred a 3D high-resolution spoiled gradient with fat suppression for imaging of the cartilage. On this sequence cartilage is bright, hence compares well to proton density weighted Fast spin echo (FSE) and arthrography with regard to detection of lesions (100). A drawback is the low signal from joint fluid and long acquisition times. The signal of fluid can be enhanced by not spoiling the sequence.. Many variations of gradient imaging have been developed like dual echo steady state imaging that has proven useful for the evaluation of cartilage morphology(97). 3D sequences have been used to evaluate total joint cartilage in pharmaceutical trials and osteoarthritis monitoring. Another method to visualize diseased cartilage is the delayed contrast enhancement. After an intravenous administration of contrast there will be a passive diffusion of contrast into the joint fluid. The negative charged gadolinium contrast molecule will diffuse into the cartilage matrix and be in conflict with the also negative charged glycosaminoglycans and therefore accumulate in places with decreased glycosaminoglycan content, decreasing the T1 value locally. This T1 value is measured and mapped as a coloured overlay on anatomic

images(101). Higher doses of gadolinium and longer delay are used compared to conventional MRI perfusion arthrography. Variations of gadolinium uptake can occur in early degeneration, but also vary after exercise and due to age, and body mass index. This method has potential to monitor the glycosaminoglycan content under treatment or for monitoring disease(102). Other MRI properties of cartilage can also be measured and displayed as an overlay like magnetization transfer contrast and apparent diffusion coefficients, both giving additional information about tissue ultrastructure and both dependent on the interaction between water and macromolecules. Common for most of these methods is that they are little used and rarely in children, what we know is then often related to articular cartilage behaviour and not to epiphyseal cartilage, which has a different structure. Many methods are time consuming and not validated, and will probably not be used in paediatric imaging in the near future.

7.5.4 Bone marrow oedema-like change

In the present study, the increased signal on T2 weighted, with a corresponding low signal on T1 weighted images was termed “bone marrow oedema-like change” as its cause, or underlying mechanism remained unclear. One might speculate that the signal change represents islands of residual red marrow; however, the conversion of bone marrow typically follows a specific pattern and is relatively fast. Reconversion, on the other hand, is only seen in different disease scenarios. Considering muscle signal as an internal reference can help differentiation as the red bone marrow still contains 40% fat which increases the signal on T1 weighted sequences as compared to muscle. The conversion of cartilage to bone starts with the breakdown of macromolecules within the matrix, releasing bound water that can give rise to focal signal increase. This has been reported in knee- and ankle joints (74). Most of the increased signal on T2 weighted images was not seen in the cartilage but in the ossified bone and might represent an age specific response to biomechanical stress, e.g. a true bone marrow oedema, even though we did not find a significant relationship to the number of training sessions per week in these children. We found, during the first examination, that more than half of the children had bone marrow oedema-like change in at least one bone, and that this was reduced to 4 in 10 at the 4 years follow up. The finding seemed to peak between 9 and 16 years of age, and unlike what was seen for bony depressions, none of the lesions found initially appeared in the same location

at follow-up. The presence of bone marrow oedema is considered pathological in patients with JIA, particularly when located adjacent to a joint, and the finding may even lead to a change of therapy(27, 28, 103). It has been suggested that the presence of bone marrow oedema adjacent to a bony depression increases the likelihood of this being a true erosion (104). This assumption was not supported by our data, as bone marrow oedema-like change was found adjacent to 20 of the bony depressions noted. Further, bone marrow oedema-like change was seen on both sides of a joint in seven of our healthy individuals, a finding previously reported to represent joint pathology(93, 105, 106).

7.5.5 Joint fluid

Joint fluid measuring ≥ 2mm was found in at least one location in around half of the children in both the initial and the follow-up studies. This was unexpected as the presence of more than 2mm joint fluid is considered pathological in adults(107). In some joints like the pisotriquetral joint, a brim of ≥2mm was frequently seen, while other joints like the distal radioulnar joint rarely presented with fluid. The presence of fluid in the pisotriquetral recess has in adults been considered as highly suggestive of synovitis (108). The amount of joint fluid that is produced increases by use, nonetheless no significant correlation was found with the number of training sessions, not even after subgrouping the training sessions into hand intensive and non-intensive training sessions. The finding of so many fluid pockets in our healthy volunteers means that this finding alone cannot be used as an indicator for disease. Increased fluid around tendons in the synovial sheath was not seen, but our coronal images without the possibility of reconstructions in other planes were suboptimal.

7.5.6 Ganglion cysts

The finding of asymptomatic and sometimes transient ganglion cysts in nearly one fourth of the healthy children was unexpected. Our study shows that wrist-ganglia also are very common in children, suggestive of a normal developmental variant. We found no sex predominance, as opposed to a study on children with symptomatic wrists, where one third was reported to have at least one ganglion cyst, with a female-male ratio of 2:1(17).

Our study is, to our knowledge, the first to report the presence of ganglion cysts on MRI in a healthy paediatric population, and the first observation of regress of ganglion cysts over time in children. The fact that nearly one third of the cysts were located dorsally, and that most cysts were located at the radiocarpal joint is consistent with previous reports from adult and paediatric populations(17, 68). The individual locations of the other cysts vary more and differ for some locations from these reports, possibly illustrating that these cysts can occur in many locations. One of the cysts was located near an area of bone marrow oedema-like change, implying that this constellation is of little help to differentiate between symptomatic and asymptomatic ganglion cysts.

7.6 Clinical implications and future perspectives

The finding of multiple and often large bony depressions in healthy children (papers 1-3) complicates the assessment of true bony changes in children with arthritis. Adding a cartilage sequence may help differentiate true erosions from normal variation, particularly in the youngest children (paper 3), given that true erosions are bare areas, e.g. uncovered by cartilage. A future scoring system for erosive bone change should therefore be based on these two sequences in combination rather than on T1 weighted images alone. Moreover, future developments of MRI hard- and software may provide more sensitive cartilage sequences, thus ease the visualisation of cartilage,

Our assumption that true erosions are uncovered by cartilage has to be confirmed in future studies. Recent studies suggest that osteitis may be a precursor for erosion, or even that osteitis is the primary pathology, preceding synovitis and erosions(26, 96).

We found surprisingly high numbers of bone marrow oedema-like changes amongst healthy children (papers 1 and 4), a finding also reported by others (81). Thus, this MRI-finding alone represents no accurate marker for true pathology. The question is whether or not the lesions seen in healthy children have similar aetiology to those seen in JIA and other disease. One might speculate that lesions in healthy children are caused by mechanical stress, and represent increased water content alone, while lesions seen in arthritis represent inflammation, e.g. increased cellularity and water content. If this is the case, the increased cellularity might result in lower Apparent Diffusion Coefficient

(ADC) values, and potential signal changes on TSE diffusion techniques. Future studies may clarify.

As for the finding of more than 2 mm joint fluid; this can no longer be considered pathological. Future MRI studies, including diffusion series with ADC mapping, may help clarify whether or not imaging will be able to differentiate pathological from healthy joint fluid.

The high prevalence of ganglion cysts, with or without coexisting bone marrow oedema-like change, highlights the need for further studies. This finding alone should not be interpreted as pathology.

In clinical practice, contrast enhanced MRI-studies are often helpful to clarify whether or not pathological changes are present. In studies of healthy volunteers, the use of intravenous contrast is unethical, however, MRI sequences such as diffusion imaging with low b-values and or bi-exponential fits and multiple b-values might be able to replace intravenous contrast in the future (109). Similar, the arterial spin labelling technique has proved helpful in assessing inflammatory arthritis of the wrist(110). Future controlled cohort studies using the abovementioned methods may help differentiate normal from pathological findings.

7.7 Strengths and weaknesses

The strength of our study is the prospective design, the inclusion of a high number of healthy children and the high follow-up rate. There are, however, some limitations such as selection bias and the use of a consensus scoring, without testing the precision of the scoring system for bony depressions. However, we feel that previous, robust repeatability studies performed by part of the study group were sufficient. Secondly, we used a 1,5 rather than a 3 tesla MRI machine and a protocol without intravenous contrast, leaving some questions unanswered.

8 Conclusions

In the wrists of healthy children;

-Bony depressions resembling erosions are frequently seen on MRI

-Bony depressions, with or without sclerosis, may occasionally be seen on radiographs

-The number of bony depressions seen on MRI increases with age

-The number of bony depressions seen on radiographs is not associated with age

-Bone marrow oedema-like change is a common MRI-finding within the carpal and the proximal metacarpal bones

-Pockets of more than 2mm joint fluid are a normal finding

-The occurrence of bone marrow oedema-like change varies over time

-Joint fluid pockets of more than 2mm may be persistent over time

-Bone marrow oedema-like change can be seen adjacent to bony depressions, ganglion cysts, and on both sides of a joint, hence, these features cannot be used in clinical practice to differentiate between pathological or normal joints, bony depressions, or ganglion cysts

-Ganglion cysts represent normal findings and occur in one fourth of healthy individuals, mostly located around the radiocarpal joint

-The occurrence and location of ganglion cysts varies over time

-The number of weekly physical activity sessions is not related to the presence of bone marrow oedema-like change or joint fluid.

9 References:

1. Boavida P, Hargunani R, Owens CM, Rosendahl K. Magnetic resonance imaging and radiographic assessment of carpal depressions in children with juvenile idiopathic arthritis: normal variants or erosions? The Journal of rheumatology. 2012 Mar;39(3):645-50.
2. Avenarius DM, Ording Muller LS, Eldevik P, Owens CM, Rosendahl K. The paediatric wrist revisited--findings of bony depressions in healthy children on radiographs compared to MRI. Pediatric radiology. 2012 Jul;42(7):791-8.
3. Muller LS, Avenarius D, Damasio B, Eldevik OP, Malattia C, Lambot-Juhan K, et al. The paediatric wrist revisited: redefining MR findings in healthy children. Annals of the rheumatic diseases. 2011 Apr;70(4):605-10.
4. Keats TE, Anderson MW. Atlas of normal roentgen variants that may simulate disease. Philadelphia, Pa.: Elsevier/Saunders,; 2013 [cited.
5. Keats TE, Smith TH. An atlas of normal developmental roentgen anatomy. 2nd ed. Chicago: Year Book Medical Publishers; 1988.
6. Keats TE. Normal variants of the hand and wrist. Hand Clin. 1991 Feb;7(1):153-66.

7. Keats TE. Some new normal roentgen variants that may simulate disease. Curr Probl Diagn Radiol. 1981 May-Jun;10(3):1-52.
8. Keats TE, Joyce JM. Metaphyseal cortical irregularities in children: a new perspective on a multi-focal growth variant. Skeletal Radiol. 1984;12(2):112-8.
9. Keats TE. Some normal variants that may be mistaken for disease. Clin Imaging. 1991 Jan-Mar;15(1):1-19.
10. Keats TE, Harrison RB. The epiphyseal spur. Skeletal Radiol. 1980;5(3):175-7.
11. Malattia C, Damasio MB, Pistorio A, Ioseliani M, Vilca I, Valle M, et al. Development and preliminary validation of a paediatric-targeted MRI scoring system for the assessment of disease activity and damage in juvenile idiopathic arthritis. Annals of the rheumatic diseases. 2011 Mar;70(3):440-6.
12. Couzens G, Daunt N, Crawford R, Ross M. Positive magnetic resonance imaging findings in the asymptomatic wrist. ANZ J Surg. 2014 Jul-Aug;84(7-8):528-32.
13. Fredericson M, Ho C, Waite B, Jennings F, Peterson J, Williams C, et al. Magnetic resonance imaging abnormalities in the shoulder and wrist joints of asymptomatic elite athletes. PM R. 2009 Feb;1(2):107-16.
14. Savnik A, Malmskov H, Thomsen HS, Graff LB, Nielsen H, Danneskiold-Samsoe B, et al. Magnetic resonance imaging of the wrist and finger joints in patients with inflammatory joint diseases. The Journal of rheumatology. 2001 Oct;28(10):2193-200.
15. Pierre-Jerome C, Moncayo V, Albastaki U, Terk MR. Multiple occult wrist bone injuries and joint effusions: prevalence and distribution on MRI. Emerg Radiol. 2010 May;17(3):179-84.
16. Razek AA, Fouda NS, Elmetwaley N, Elbogdady E. Sonography of the knee joint(). J Ultrasound. 2009 Jun;12(2):53-60.
17. Bracken J, Bartlett M. Ganglion cysts in the paediatric wrist: magnetic resonance imaging findings. Pediatric radiology. 2013 Dec;43(12):1622-8.
18. Stelling CB, Keats MM, Keats TE. Irregularities at the base of the proximal phalanges: false indicator of early rheumatoid arthritis. AJR American journal of roentgenology. 1982 Apr;138(4):695-8.
19. Parodi M, Silvestri E, Garlaschi G, Cimmino MA. How normal are the hands of normal controls? A study with dedicated magnetic resonance imaging. Clin Exp Rheumatol. 2006 Mar-Apr;24(2):134-41.
20. De Zwart AD, Beeres FJ, Ring D, Kingma LM, Coerkamp EG, Meylaerts SA, et al. MRI as a reference standard for suspected scaphoid fractures. Br J Radiol. 2012 Aug;85(1016):1098-101.
21. Prakken B, Albani S, Martini A. Juvenile idiopathic arthritis. Lancet. 2011 Jun 18;377(9783):2138-49.
22. Berntson L, Andersson Gare B, Fasth A, Herlin T, Kristinsson J, Lahdenne P, et al. Incidence of juvenile idiopathic arthritis in the Nordic countries. A population based study with special reference to the validity of the ILAR and EULAR criteria. The Journal of rheumatology. 2003 Oct;30(10):2275-82.
23. Petty RE, Southwood TR, Manners P, Baum J, Glass DN, Goldenberg J, et al. International League of Associations for Rheumatology classification of juvenile idiopathic arthritis: second revision, Edmonton, 2001. The Journal of rheumatology. 2004 Feb;31(2):390-2.

24. Ravelli A, Martini A. Juvenile idiopathic arthritis. Lancet. 2007 Mar 3;369(9563):767-78.
25. Levick JR. Permeability of rheumatoid and normal human synovium to specific plasma proteins. Arthritis and rheumatism. 1981 Dec;24(12):1550-60.
26. McQueen FM. Bone marrow edema and osteitis in rheumatoid arthritis: the imaging perspective. Arthritis research & therapy. 2012;14(5):224.
27. Sheybani EF, Khanna G, White AJ, Demertzis JL. Imaging of juvenile idiopathic arthritis: a multimodality approach. Radiographics : a review publication of the Radiological Society of North America, Inc. 2013 Sep-Oct;33(5):1253-73.
28. Johnson K. Imaging of juvenile idiopathic arthritis. Pediatric radiology. 2006 Aug;36(8):743-58.
29. Ravelli A, Ioseliani M, Norambuena X, Sato J, Pistorio A, Rossi F, et al. Adapted versions of the Sharp/van der Heijde score are reliable and valid for assessment of radiographic progression in juvenile idiopathic arthritis. Arthritis and rheumatism. 2007 Sep;56(9):3087-95.
30. Rossi F, Di Dia F, Galipo O, Pistorio A, Valle M, Magni-Manzoni S, et al. Use of the Sharp and Larsen scoring methods in the assessment of radiographic progression in juvenile idiopathic arthritis. Arthritis and rheumatism. 2006 Oct 15;55(5):717-23.
31. Poznanski AK, Hernandez RJ, Guire KE, Bereza UL, Garn SM. Carpal length in children--a useful measurement in the diagnosis of rheumatoid arthritis and some concenital malformation syndromes. Radiology. 1978 Dec;129(3):661-8.
32. Malattia C, Damasio MB, Magnaguagno F, Pistorio A, Valle M, Martinoli C, et al. Magnetic resonance imaging, ultrasonography, and conventional radiography in the assessment of bone erosions in juvenile idiopathic arthritis. Arthritis and rheumatism. 2008 Dec 15;59(12):1764-72.
33. Emery KH. MR imaging in congenital and acquired disorders of the pediatric upper extremity. Magn Reson Imaging Clin N Am. 2009 Aug;17(3):549-70, vii.
34. Kerssemakers SP, Fotiadou AN, de Jonge MC, Karantanas AH, Maas M. Sport injuries in the paediatric and adolescent patient: a growing problem. Pediatric radiology. 2009 May;39(5):471-84.
35. Dwek JR, Cardoso F, Chung CB. MR imaging of overuse injuries in the skeletally immature gymnast: spectrum of soft-tissue and osseous lesions in the hand and wrist. Pediatric radiology. 2009 Dec;39(12):1310-6.
36. Dodwell ER. Osteomyelitis and septic arthritis in children: current concepts. Curr Opin Pediatr. 2013 Feb;25(1):58-63.
37. Blickman JG, van Die CE, de Rooy JW. Current imaging concepts in pediatric osteomyelitis. European radiology. 2004 Mar;14 Suppl 4:L55-64.
38. Wihlborg C, Babyn P, Ranson M, Laxer R. Radiologic mimics of juvenile rheumatoid arthritis. Pediatric radiology. 2001 May;31(5):315-26.
39. Kandel L, Friedman A, Chaimski G, Howard C, Mann G, Lowe J. Foreign-body synovitis mimicking septic arthritis of the knee. Arthroscopy. 2001 Nov-Dec;17(9):993-6.
40. Huber AM, Lam PY, Duffy CM, Yeung RS, Ditchfield M, Laxer D, et al. Chronic recurrent multifocal osteomyelitis: clinical outcomes after more than five years of follow-up. J Pediatr. 2002 Aug;141(2):198-203.
41. Iyer RS, Thapa MM, Chew FS. Chronic recurrent multifocal osteomyelitis: review. AJR American journal of roentgenology. 2011 Jun;196(6 Suppl):S87-91.

42. Robertson LP, Hickling P. Chronic recurrent multifocal osteomyelitis is a differential diagnosis of juvenile idiopathic arthritis. Annals of the rheumatic diseases. 2001 Sep;60(9):828-31.
43. Plesca DA, Luminos M, Spatariu L, Stefanescu M, Cinteza E, Balgradean M. Postinfectious arthritis in pediatric practice. Maedica (Buchar). 2013 Jun;8(2):164-9.
44. Arkader A, Brusalis C, Warner WC, Jr., Conway JH, Noonan K. Update in Pediatric Musculoskeletal Infections: When It Is, When It Isn't, and What to Do. J Am Acad Orthop Surg. 2016 Sep;24(9):e112-21.
45. Lancourt JE, Gilbert MS, Posner MA. Management of bleeding and associated complications of hemophilia in the hand and forearm. J Bone Joint Surg Am. 1977 Jun;59(4):451-60.
46. Chan MW, Leckie A, Xavier F, Uleryk E, Tadros S, Blanchette V, et al. A systematic review of MR imaging as a tool for evaluating haemophilic arthropathy in children. Haemophilia. 2013 Nov;19(6):e324-34.
47. Doria AS. State-of-the-art imaging techniques for the evaluation of haemophilic arthropathy: present and future. Haemophilia. 2010 Jul;16 Suppl 5:107-14.
48. Poonnoose PM, Hilliard P, Doria AS, Keshava SN, Gibikote S, Kavitha ML, et al. Correlating clinical and radiological assessment of joints in haemophilia: results of a cross sectional study. Haemophilia. 2016 Nov;22(6):925-33.
49. Murphey MD, Rhee JH, Lewis RB, Fanburg-Smith JC, Flemming DJ, Walker EA. Pigmented villonodular synovitis: radiologic-pathologic correlation. Radiographics : a review publication of the Radiological Society of North America, Inc. 2008 Sep-Oct;28(5):1493-518.
50. Mukhopadhyay K, Smith M, Hughes PM. Multifocal PVNS in a child--followed over 25 years. Skeletal Radiol. 2006 Jul;35(7):539-42.
51. Maurice H, Crone M, Watt I. Synovial chondromatosis. J Bone Joint Surg Br. 1988 Nov;70(5):807-11.
52. Murphey MD, Vidal JA, Fanburg-Smith JC, Gajewski DA. Imaging of synovial chondromatosis with radiologic-pathologic correlation. Radiographics : a review publication of the Radiological Society of North America, Inc. 2007 Sep-Oct;27(5):1465-88.
53. Hospach T, Langendorfer M, Kalle TV, Tewald F, Wirth T, Dannecker GE. Mimicry of lyme arthritis by synovial hemangioma. Rheumatology international. 2011 Dec;31(12):1639-43.
54. Christodoulou A, Ploumis A, Karkavelas G, Terzidis I, Tsagias I. A rare case of juxtaarticular osteoid osteoma of the calcaneus initially misdiagnosed as juvenile chronic arthritis. Arthritis and rheumatism. 2003 Mar;48(3):776-9.
55. Uhl M, Herget G, Kurz P. [Cartilage tumors : Pathology and radiomorphology]. Radiologe. 2016 Jun;56(6):476-88.
56. Hoover KB, Rosenthal DI, Mankin H. Langerhans cell histiocytosis. Skeletal Radiol. 2007 Feb;36(2):95-104.
57. Davies AM, Grainger AJ, James SJ, SpringerLink (Online service). Imaging of the Hand and Wrist Techniques and Applications. Berlin, Heidelberg: Springer Berlin Heidelberg : Imprint: Springer,; 2013 [cited.
58. Pyle SI, Waterhouse AM, Greulich WW. Attributes of the radiographic standard of reference for the National Health Examination Survey. Am J Phys Anthropol. 1971 Nov;35(3):331-7.

59. Bull RK, Edwards PD, Kemp PM, Fry S, Hughes IA. Bone age assessment: a large scale comparison of the Greulich and Pyle, and Tanner and Whitehouse (TW2) methods. Arch Dis Child. 1999 Aug;81(2):172-3.
60. Canovas F, Banegas F, Cyteval C, Jaeger M, DiMeglio A, Bonnel F, et al. Carpal bone maturation assessment by image analysis from computed tomography scans. Horm Res. 2000;54(1):6-13.
61. Greulich WW, Pyle SI. Radiographic atlas of skeletal development of the hand and wrist. 2d ed. Stanford, Calif.,: Stanford Univ. Press; 1959.
62. Smith MD. The normal synovium. Open Rheumatol J. 2011;5:100-6.
63. Levick JR, McDonald JN. Fluid movement across synovium in healthy joints: role of synovial fluid macromolecules. Annals of the rheumatic diseases. 1995 May;54(5):417-23.
64. Jay GD, Britt DE, Cha CJ. Lubricin is a product of megakaryocyte stimulating factor gene expression by human synovial fibroblasts. The Journal of rheumatology. 2000 Mar;27(3):594-600.
65. Morrison WB. Indirect MR arthrography: concepts and controversies. Semin Musculoskelet Radiol. 2005 Jun;9(2):125-34.
66. Loredo RA, Sorge DG, Garcia G. Radiographic evaluation of the wrist: a vanishing art. Semin Roentgenol. 2005 Jul;40(3):248-89.
67. Theumann NH, Pfirrmann CW, Chung CB, Antonio GE, Trudell DJ, Resnick D. Pisotriquetral joint: assessment with MR imaging and MR arthrography. Radiology. 2002 Mar;222(3):763-70.
68. Lowden CM, Attiah M, Garvin G, Macdermid JC, Osman S, Faber KJ. The prevalence of wrist ganglia in an asymptomatic population: magnetic resonance evaluation. J Hand Surg Br. 2005 Jun;30(3):302-6.
69. Angelides AC, Wallace PF. The dorsal ganglion of the wrist: its pathogenesis, gross and microscopic anatomy, and surgical treatment. J Hand Surg Am. 1976 Nov;1(3):228-35.
70. Smith PLG. Tumours benign swelling and ulceration. In: Lister G, editor. The hand: diagnosis and indications. Edinburgh ; New York: Churchill Livingstone; 1977. p. xi, 224 p.
71. Loder RT, Robinson JH, Jackson WT, Allen DJ. A surface ultrastructure study of ganglia and digital mucous cysts. J Hand Surg Am. 1988 Sep;13(5):758-62.
72. Murray PM. Ganglion Cysts in the Wrist. In: Cooney WP, Linscheid RL, editors. The Wrist : diagnosis and operative treatment. St. Louis: Mosby; 1998.
73. Khanna PC, Thapa MM. The growing skeleton: MR imaging appearances of developing cartilage. Magn Reson Imaging Clin N Am. 2009 Aug;17(3):411-21, v.
74. Jaimes C, Chauvin NA, Delgado J, Jaramillo D. MR imaging of normal epiphyseal development and common epiphyseal disorders. Radiographics : a review publication of the Radiological Society of North America, Inc. 2014 Mar-Apr;34(2):449-71.
75. Thapa MM, Iyer RS, Khanna PC, Chew FS. MRI of pediatric patients: Part 1, normal and abnormal cartilage. AJR American journal of roentgenology. 2012 May;198(5):W450-5.
76. Shabshin N, Schweitzer ME, Morrison WB, Carrino JA, Keller MS, Grissom LE. High-signal T2 changes of the bone marrow of the foot and ankle in children: red marrow or traumatic changes? Pediatric radiology. 2006 Jul;36(7):670-6.

77. Jaimes C, Jimenez M, Marin D, Ho-Fung V, Jaramillo D. The trochlear pre-ossification center: a normal developmental stage and potential pitfall on MR images. Pediatric radiology. 2012 Nov;42(11):1364-71.
78. Jans LB, Jaremko JL, Ditchfield M, Verstraete KL. Evolution of femoral condylar ossification at MR imaging: frequency and patient age distribution. Radiology. 2011 Mar;258(3):880-8.
79. McNeilly CM, Banes AJ, Benjamin M, Ralphs JR. Tendon cells in vivo form a three dimensional network of cell processes linked by gap junctions. J Anat. 1996 Dec;189 (Pt 3):593-600.
80. Curry TS, Dowdey JE, Murry RC, Christensen EE. Christensen's physics of diagnostic radiology. 4th ed. Philadelphia: Lea & Febiger; 1990.
81. Shabshin N, Schweitzer ME. Age dependent T2 changes of bone marrow in pediatric wrist MRI. Skeletal Radiol. 2009 Dec;38(12):1163-8.
82. Altman DG. Practical statistics for medical research. London ; New York: Chapman and Hall; 1991.
83. Bland M. An introduction to medical statistics. 3rd ed. Oxford ; New York: Oxford University Press; 2000.
84. Chow S-C, Shao J, Wang H. Sample size calculations in clinical research. New York: Marcel Dekker,; 2003 [cited.
85. Thodberg HH, Kreiborg S, Juul A, Pedersen KD. The BoneXpert method for automated determination of skeletal maturity. IEEE transactions on medical imaging. 2009 Jan;28(1):52-66.
86. Tanturri de Horatio L, Damasio MB, Barbuti D, Bracaglia C, Lambot-Juhan K, Boavida P, et al. MRI assessment of bone marrow in children with juvenile idiopathic arthritis: intra- and inter-observer variability. Pediatric radiology. 2012 Jun;42(6):714-20.
87. Hardyck C, Petrinovich LF. Left-handedness. Psychol Bull. 1977 May;84(3):385-404.
88. Boavida P, Lambot-Juhan K, Muller LS, Damasio B, de Horatio LT, Malattia C, et al. Carpal erosions in children with juvenile idiopathic arthritis: repeatability of a newly devised MR-scoring system. Pediatric radiology. 2015 Dec;45(13):1972-80.
89. Bankier AA, Levine D, Halpern EF, Kressel HY. Consensus interpretation in imaging research: is there a better way? Radiology. 2010 Oct;257(1):14-7.
90. Espeland A, Vetti N, Krakenes J. Are two readers more reliable than one? A study of upper neck ligament scoring on magnetic resonance images. BMC Med Imaging. 2013 Jan 17;13:4.
91. Edwards SD, McNamee MJ. Ethical concerns regarding guidelines for the conduct of clinical research on children. Journal of medical ethics. 2005 Jun;31(6):351-4.
92. Palosaari K, Vuotila J, Soini I, Kaarela K, Kautiainen H, Hakala M. Small bone lesions resembling erosions can frequently be found in bilateral wrist MRI of healthy individuals. Scand J Rheumatol. 2009 Nov-Dec;38(6):450-4.
93. Jimenez-Boj E, Nobauer-Huhmann I, Hanslik-Schnabel B, Dorotka R, Wanivenhaus AH, Kainberger F, et al. Bone erosions and bone marrow edema as defined by magnetic resonance imaging reflect true bone marrow inflammation in rheumatoid arthritis. Arthritis and rheumatism. 2007 Apr;56(4):1118-24.

94. Gravallese EM, Harada Y, Wang JT, Gorn AH, Thornhill TS, Goldring SR. Identification of cell types responsible for bone resorption in rheumatoid arthritis and juvenile rheumatoid arthritis. Am J Pathol. 1998 Apr;152(4):943-51.
95. Boyesen P, Haavardsholm EA, Ostergaard M, van der Heijde D, Sesseng S, Kvien TK. MRI in early rheumatoid arthritis: synovitis and bone marrow oedema are independent predictors of subsequent radiographic progression. Annals of the rheumatic diseases. 2011 Mar;70(3):428-33.
96. Schett G, Firestein GS. Mr Outside and Mr Inside: classic and alternative views on the pathogenesis of rheumatoid arthritis. Annals of the rheumatic diseases. 2010 May;69(5):787-9.
97. Gold GE, Chen CA, Koo S, Hargreaves BA, Bangerter NK. Recent advances in MRI of articular cartilage. AJR American journal of roentgenology. 2009 Sep;193(3):628-38.
98. Ronga M, Angeretti G, Ferraro S, G DEF, Genovese EA, Cherubino P. Imaging of articular cartilage: current concepts. Joints. 2014 Jul-Sep;2(3):137-40.
99. Hani AF, Kumar D, Malik AS, Ahmad RM, Razak R, Kiflie A. Non-invasive and in vivo assessment of osteoarthritic articular cartilage: a review on MRI investigations. Rheumatology international. 2015 Jan;35(1):1-16.
100. Link TM, Stahl R, Woertler K. Cartilage imaging: motivation, techniques, current and future significance. European radiology. 2007 May;17(5):1135-46.
101. Gold GE, McCauley TR, Gray ML, Disler DG. What's new in cartilage? Radiographics : a review publication of the Radiological Society of North America, Inc. 2003 Sep-Oct;23(5):1227-42.
102. Crema MD, Roemer FW, Marra MD, Burstein D, Gold GE, Eckstein F, et al. Articular cartilage in the knee: current MR imaging techniques and applications in clinical practice and research. Radiographics : a review publication of the Radiological Society of North America, Inc. 2011 Jan-Feb;31(1):37-61.
103. Breton S, Jousse-Joulin S, Finel E, Marhadour T, Colin D, de Parscau L, et al. Imaging approaches for evaluating peripheral joint abnormalities in juvenile idiopathic arthritis. Semin Arthritis Rheum. 2012 Apr;41(5):698-711.
104. Kan JH. Juvenile idiopathic arthritis and enthesitis-related arthropathies. Pediatric radiology. 2013 Mar;43 Suppl 1:S172-80.
105. Lisbona MP, Pamies A, Ares J, Almirall M, Navallas M, Solano A, et al. Association of bone edema with the progression of bone erosions quantified by hand magnetic resonance imaging in patients with rheumatoid arthritis in remission. The Journal of rheumatology. 2014 Aug;41(8):1623-9.
106. Sudol-Szopinska I, Kontny E, Maslinski W, Prochorec-Sobieszek M, Warczynska A, Kwiatkowska B. Significance of bone marrow edema in pathogenesis of rheumatoid arthritis. Pol J Radiol. 2013 Jan;78(1):57-63.
107. Ejbjerg B, McQueen F, Lassere M, Haavardsholm E, Conaghan P, O'Connor P, et al. The EULAR-OMERACT rheumatoid arthritis MRI reference image atlas: the wrist joint. Annals of the rheumatic diseases. 2005 Feb;64 Suppl 1:i23-47.
108. Barakat MS, Schweitzer ME, Morisson WB, Culp RW, Bordalo-Rodrigues M. Reactive carpal synovitis: initial experience with MR imaging. Radiology. 2005 Jul;236(1):231-6.
109. Neubauer H, Evangelista L, Morbach H, Girschick H, Prelog M, Kostler H, et al. Diffusion-weighted MRI of bone marrow oedema, soft tissue oedema and synovitis in paediatric patients: feasibility and initial experience. Pediatr Rheumatol Online J. 2012;10(1):20.

110. Boss A, Martirosian P, Fritz J, Kotter I, Henes JC, Claussen CD, et al. Magnetic resonance spin-labeling perfusion imaging of synovitis in inflammatory arthritis at 3.0 T. MAGMA. 2009 Jun;22(3):175-80.

Paper I

Paper II

Paper III

Paper IV

Appendix

Forespørsel om deltakelse i forskningsprosjektet

"Ussurer i håndrotsben hos barn med leddgikt, normalt funn eller sykdom?"

Bakgrunn og hensikt
Dette er et spørsmål til deg og ditt barn om deltakelse i en forskningsstudie hvor vi ønsker å studere hender hos friske barn. Dette for å kunne tolke røntgenfunn hos pasienter med barneleddgikt slik at vi kan skille tidlige røntgenforandringer som skyldes sykdom fra normale funn. Studien vil foregå ved Røntgenavdelingen, UNN Tromsø og er et ledd i en større internasjonal studie. Deltakelse er helt frivillig.

Hva innebærer studien?
I studien ønsker vi å undersøke venstre hånd på friske barn i aldersgruppen **6- 14** år. Vi vil undersøke hånden med en MR- sekvens og et røntgenbilde. Barnet må ligge på MR- benken i ca to minutter og stikke hånden inn i MR- maskinen. Etterpå vil vi ta et røntgenbilde av hånden. Foreldre eller annen voksenperson kan være med hele tiden.
Vi ønsker også å vite barnets eksakte alder, høyde, vekt, og eventuelle tidligere sykdommer.

Mulige fordeler og ulemper
MR- maskinen bråker litt og selve maskinen vil kunne virke skremmende. Dette oppleves imidlertid svært sjelden som et problem i den aldersgruppen vi ønsker å undersøke. Barnet vil få god informasjon og kan ha med seg foresatt eller annen voksenperson.
Vi vil også ta røntgenbilde av hånden. Bruk av røntgenstråler kan være forbundet med medisinsk risiko. Den dosen barnet får er imidlertid så liten at det ikke er målbar risiko ved undersøkelsen.

Hva skjer med informasjonen om barnet?
Prøvene tatt av barnet og informasjonen som registreres skal kun brukes slik som beskrevet i hensikten med studien. Alle opplysningene og prøvene vil bli behandlet uten navn og fødselsnummer eller andre direkte gjenkjennende opplysninger. En kode knytter personopplysningene til barnets bilder. Det er kun autorisert personell knyttet til prosjektet som har adgang til listen og som kan finne tilbake til barnet. Det vil ikke være mulig å identifisere barnet i resultatene av studien når disse publiseres.

Frivillig deltakelse
Det er frivillig å delta i studien. Dersom barnet blir engstelig eller vegrer seg underveis avslutter vi undersøkelsen. Dere kan når som helst og uten å oppgi noen grunn trekke deres samtykke til å la barnet delta i studien.
Dersom du og barnet ønsker å delta, undertegner du/dere samtykkeerklæringen på siste side. Om dere nå sier ja til å delta, kan dere senere trekke tilbake samtykke. Dersom dere senere ønsker å trekke dere eller har spørsmål til studien, kan dere kontakte Lil-Sofie Ording Müller, konstituert overlege, Radiologisk avdeling UNN, Tlf: 77628306., e- post: lil-sofie.ording.muller@unn.no.

Ytterligere informasjon om studien finnes i kapittel ***A*** *– utdypende forklaring av hva studien innebærer.*
Ytterligere informasjon om, personvern og forsikring finnes i kapittel B *– Personvern, økonomi og forsikring.*

Samtykkeerklæring følger etter kapittel B.

Kapittel A- utdypende forklaring av hva studien innebærer

Vi ønsker å undersøke venstre hånd hos barn mellom 6 og 14 år. Nye røntgen og MR- teknikker (Magnet Tomografi- teknikker) gjør det nå mulig å finne små forandringer i skjelettet hos pasienter med barneleddgikt. Dersom man finner forandringene tidlig hos disse pasientene vil man kunne sette inn behandlingstiltak som hemmer utviklingen av sykdom. Problemet er imidlertid at man ikke er sikre på om de minste forandringene virkelig er et uttrykk for sykdom eller om dette er funn som også finnes hos friske barn, altså normalfunn. Derfor ønsker vi å kartlegge venstre hånd hos ca 80 friske barn mellom 6 og 14 år med en MR- sekvens og et røntgenbilde for å sammenlikne bildene fra friske barn med bildene fra barn med barneleddgikt.

For at barnet skal kunne være med i studien må han/hun ikke ha noen alvorlige eller kroniske sykdommer. Barnet må ikke ha metallproteser eller implantater, eller ha pacemaker.

Barnet skal ligge med hånden inn i MR- maskinen og selve billedopptaket tar ca to minutter. Når billedopptaket foregår må barnet ha hånden i ro. Det medfører ikke fare å røre på hånden, men bildene kan bli mislykket. Foresatte eller annen voksenperson kan være tilstede under hele undersøkelsen. MR- maskinen bråker de to minuttene det tar mens billedopptaket foregår. Barnet vil da ha på seg øreklokker og eventuelt høre på musikk.
Etterpå tas et vanlig røntenbilde av hånden. Vi vil også veie og måle barnet og vite fødselsdato og eventuelle tildligere sykdommer. Hele undersøkelsen (fra dere kommer til Røntgenavdelingen til dere kan dra hjem) vil ta ca en halv time.

Undersøkelsen vil foregå i løpet av våren og høsten 2009. Vi vil avtale oppmøtetidspunkt og oppmøtested med dere direkte. Undersøkelsen vil foregå på Røntgenavdelingen på UNN.

Det kan tenkes at barnet vil kunne føle undersøkelsessituasjonen som uvant og litt skremmende. Det pleier imidlertid ikke å være noe problem i aldersgruppen 6- 14 år. Barnet vil få god informasjon om hva som skal foregå og foresatte eller annen voksenperson kan være med hele tiden. Dere eller barnet vil kunne avbryte undersøkelsen når som helst. Selve billedopptaket tar kort tid (2 min MR, sekunder på rtg).

Både røntgen og MR er vel utprøvde medisinsk- diagnostiske metoder. MR har ingen kjente bivirkninger. Bruk av røntgenstråler har potensielt medisinske skadevirkninger. Den mengden røntgenstråler barnet får ved deltakelse i denne studien er imidlertid så liten at det medfører ingen fare. Stråledosen tilsvarer ca 5 timer normal bakgrunnsstråling (den strålingen vi normalt omgir oss med i hverdagen) og medfører ingen påvisbar økt risiko for sykdom eller skade.

Dersom barnet blir engstelig eller vegrer seg underveis vil vi avbryte undersøkelsen.

Kapittel B - Personvern, økonomi og forsikring

Personvern
Opplysninger som registreres om barnet er røntgen- og MR- bildene av ve hånd. Disse vil bli lagret i UNN sin røntgenjournal (IMPAX). I tillegg vil informasjonen du gir oss om barnets høyde, vekt og eventuelle tidligere sykdommer bli lagret **avidentifisert** som konfidensielle opplysninger i en forskningsperm. Bildene vil bli liggende i IMPAX mens opplysningene vil bli makulert når dataene er ferdig bearbeidet.

Det er kun de som gjennomfører studien som vil få tilgang på opplysningene, overlege Lil-Sofie Ording Müller (UNN) og overlege Derk Avenarius (UNN). Overlege Karen Rosendahl (Great Ormond Street Hospital for Children), vil se på bildene, **avidentifisert.**

Universitetssykehuset Nord Norge ved administrerende direktør er databehandlingsansvarlig.

Utlevering av materiale og opplysninger til andre
Hvis du og barnet sier ja til å delta i studien, gir du også ditt samtykke til at **avidentifiserte** bilder og **avidentifiserte** opplysninger utleveres Great Ormond Street Hospital for Children, London, England.

Rett til innsyn og sletting av opplysninger om deg og sletting av prøver
Hvis du og ditt barn sier ja til å delta i studien, har du rett til å få innsyn i hvilke opplysninger som er registrert om barnet. Dere har videre rett til å få korrigert eventuelle feil i de opplysningene vi har registrert. Dersom dere trekker dere fra studien, kan dere kreve å få slettet innsamlede prøver og opplysninger, med mindre opplysningene allerede er inngått i analyser eller brukt i vitenskapelige publikasjoner.

Økonomi og UNNs rolle
Studien er finansiert gjennom forskningsmidler fra UNN. Det er ingen økonomisk gevinst for UNN eller legene som gjennomfører denne studien.

Forsikring
Pasientskadeerstatningsordningen

Informasjon om utfallet av studien
Alle som deltar kan få informasjon om utfallet av studien dersom de ønsker det.

Samtykke til deltakelse i studien

Jeg er villig til å la mitt barn delta i studien

(Signert av foresatt, dato, sigenres uansett alder på barnet)

Deltakers navn, evt underskrift dersom barnet er over 12 år:

(Signeres også av barnet dersom barnet er over 12 år)

Jeg bekrefter å ha gitt informasjon om studien

(Signert, rolle i studien, dato)

HEI! *16.03.09*

Vi er to doktorer som lurer på om vi kan få ta bilde av deg med vår MR- maskin. Vi vil nemlig se på bilder av friske barn. På den måten kan vi lære mer om menneskekroppen og det er viktig når man er doktor.

Det er en stor maskin som bråker litt, men den er ikke farlig. Hvis du vil kan du høre på musikk mens vi tar bildene og du kjenner ingen ting.

Du får lov til å ha med deg en voksen hele tiden.

Du kan snakke og røre på deg inne i MR- rommet, men i tre minutter må du ligge helt stille for at vi skal få fine bilder.

Du kan spørre oss hvis det er noe du lurer på.

Vi blir veldig glad hvis du vil delta i undersøkelsen vår men det er helt frivillig. Hvis du vil bli med men ombestemmer deg underveis er dette også helt greit!

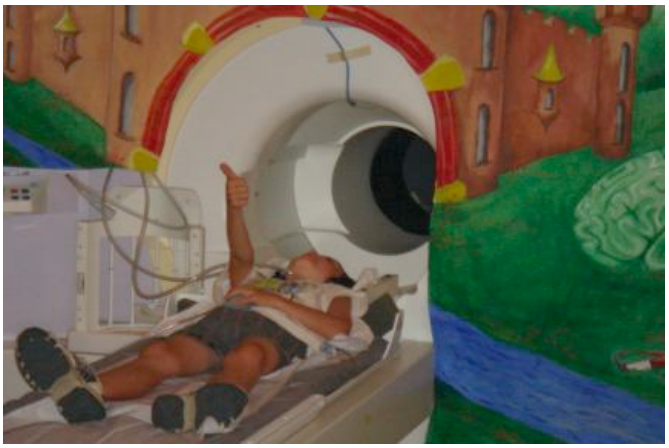

Hilsen dr. Lil-Sofie Ording Müller og dr. Derk Avenarius.

REGISTRERINGSSKJEMA – HÅNDSTUDIE/DWIBS

Aksesjonsnummer:……

Fødselsdato:…… Kjønn: M / K

Tidligere sykdommer:……
……
……
……
……
……

Medikamenter:……
……
……

Høyde:……..

Vekt:…….

Er MR- sjekkliste fylt ut?

Forespørsel om deltakelse i forskningsprosjektet

"Ussurer i håndrotsben hos barn med leddgikt, normalt funn eller sykdom en oppfølgings studie"

Bakgrunn og hensikt
Dette er et spørsmål til deg og ditt barn om deltakelse i en forskningsstudie hvor vi ønsker å studere hender hos friske barn. Dette for å kunne tolke røntgenfunn hos pasienter med barneleddgikt slik at vi kan skille tidlige røntgenforandringer som skyldes sykdom fra normale funn. Studien vil foregå ved Røntgenavdelingen, UNN Tromsø og er et ledd i en større internasjonal studie. Deltakelse er helt frivillig.

Hva innebærer studien?
I studien ønsker vi igjen å undersøke venstre hånd på 89 friske barn som deltok i en kartleggingsundersøkelse i 2009\2010. Dette vil skje på akkurat samme måte som sist. Vi vil undersøke hånden med en MR- sekvens og et røntgenbilde. Barnet må ligge på MR- benken i ca 10 minutter og stikke hånden inn i MR- maskinen. Etterpå vil vi ta et røntgenbilde av hånden. Foreldre eller annen voksenperson kan være med hele tiden.
Vi ønsker også å vite barnets eksakte alder, høyde, vekt, og eventuelle tidligere sykdommer. Vi vil spørre om barnet er høyre eller venstre hendt og om det har skadet seg i det siste. Vi vil også spørre om idretsaktiviteter.

Mulige fordeler og ulemper
MR- maskinen bråker litt og selve maskinen vil kunne virke skremmende. Dette oppleves imidlertid svært sjelden som et problem i den aldersgruppen vi ønsker å undersøke. Barnet vil få god informasjon og kan ha med seg foresatt eller annen voksenperson.
Vi vil også ta røntgenbilde av hånden. Bruk av røntgenstråler kan være forbundet med medisinsk risiko. Den dosen barnet får er imidlertid så liten at det ikke er målbar risiko ved undersøkelsen.

Hva skjer med informasjonen om barnet?
Prøvene tatt av barnet og informasjonen som registreres skal kun brukes slik som beskrevet i hensikten med studien. Alle opplysningene og prøvene vil bli behandlet uten navn og fødselsnummer eller andre direkte gjenkjennende opplysninger. En kode knytter personopplysningene til barnets bilder. Det er kun autorisert personell knyttet til prosjektet som har adgang til listen og som kan finne tilbake til barnet. Det vil ikke være mulig å identifisere barnet i resultatene av studien når disse publiseres.

Frivillig deltakelse
Det er frivillig å delta i studien. Dersom barnet blir engstelig eller vegrer seg underveis avslutter vi undersøkelsen. Dere kan når som helst og uten å oppgi noen grunn trekke deres samtykke til å la barnet delta i studien.
Dersom du og barnet ønsker å delta, undertegner du/dere samtykkeerklæringen på siste side. Om dere nå sier ja til å delta, kan dere senere trekke tilbake samtykke. Dersom dere senere ønsker å trekke dere eller har spørsmål til studien, kan dere kontakte Derk Avenarius overlege, Radiologisk avdeling UNN, Tlf: 77628406., e- post: derk.avenarius@unn.no.

Ytterligere informasjon om studien finnes i kapittel *A* *– utdypende forklaring av hva studien innebærer.*
Ytterligere informasjon om, personvern og forsikring finnes i kapittel B *– Personvern, økonomi og forsikring.*

Samtykkeerklæring følger etter kapittel B.

Kapittel A- utdypende forklaring av hva studien innebærer

Vi har i 2009\2010 undersøkt venstre hånd hos 89 barn mellom 6 og 16 år. Dette har skapt ny innsikt i hvordan disse bildene må tolkes hos syke og friske barn. Resultatene er publisert i internasjonale fag tidsskrifter og har gitt en bedre forståelse av skjelett modning hos barn. Nye røntgen og MR-teknikker (Magnet Tomografi- teknikker) gjør det nå mulig å finne små forandringer i skjelettet hos pasienter med barneleddgikt. Dersom man finner forandringene tidlig hos disse pasientene vil man kunne sette inn behandlingstiltak som hemmer utviklingen av sykdom. Problemet er imidlertid at man ikke er sikre på om de minste forandringene virkelig er et uttrykk for sykdom eller om dette er funn som også finnes hos friske barn, altså normalfunn. Det er heller ingen som har sett på skjelettmodning med MR over tid .Derfor ønsker vi igjen å kartlegge venstre hånd hos 89 friske barn som ble skannet tidligere med en MR- sekvens og et røntgenbilde for å sammenlikne disse bildene med bildene som er tatt tidligere og også for å sammenligne med bilder fra barn med barneleddgikt.

For at barnet skal kunne være med i studien må han/hun ikke ha noen alvorlige eller kroniske sykdommer. Barnet må ikke ha metallproteser eller implantater, eller ha pacemaker.

Barnet skal ligge med hånden inn i MR- maskinen og selve billedopptaket tar ca to ganger 4 minutter. Når billedopptaket foregår må barnet ha hånden i ro. Det medfører ikke fare å røre på hånden, men bildene kan bli mislykket. Foresatte eller annen voksenperson kan som før være tilstede under hele undersøkelsen. MR- maskinen bråker de minuttene det tar mens billedopptaket foregår. Barnet vil da ha på seg øreklokker og eventuelt høre på musikk.
Etterpå tas et vanlig røntenbilde av hånden. Vi vil også veie og måle barnet og vite fødselsdato og eventuelle tidligere sykdommer. Hele undersøkelsen (fra dere kommer til Røntgenavdelingen til dere kan dra hjem) vil ta ca en halv time.

Undersøkelsen vil foregå i løpet av våren 2013. Vi vil avtale oppmøtetidspunkt og oppmøtested med dere direkte. Undersøkelsen vil foregå på Røntgenavdelingen på UNN.

Det kan tenkes at barnet vil kunne føle undersøkelsessituasjonen som uvant og litt skremmende. Vi håper at barnet vil huske første gangen de ble undersøkt som en ikke skremmende opplevelse, og at de har lyst til å stille opp igjen. Barnet vil få god informasjon om hva som skal foregå og foresatte eller annen voksenperson kan være med hele tiden. Dere eller barnet vil kunne avbryte undersøkelsen når som helst. Selve billedopptaket tar kort tid (10 min MR, sekunder på rtg).

Både røntgen og MR er vel utprøvde medisinsk- diagnostiske metoder. MR har ingen kjente bivirkninger. Bruk av røntgenstråler har potensielt medisinske skadevirkninger. Den mengden røntgenstråler barnet får ved deltakelse i denne studien er imidlertid så liten at det medfører ingen fare. Stråledosen tilsvarer ca 5 timer normal bakgrunns stråling (den strålingen vi normalt omgir oss med i hverdagen) og medfører ingen påvisbar økt risiko for sykdom eller skade.

Dersom barnet blir engstelig eller vegrer seg underveis vil vi avbryte undersøkelsen.

Kapittel B - Personvern, økonomi og forsikring

Personvern
Opplysninger som registreres om barnet er røntgen- og MR- bildene av ve hånd. Disse vil bli lagret i UNN sin røntgenjournal (IMPAX). I tillegg vil informasjonen du gir oss om barnets høyde, vekt og

eventuelle tidligere sykdommer bli lagret **avidentifisert** som konfidensielle opplysninger i en forskningsperm. Bildene vil bli liggende i IMPAX mens opplysningene vil bli makulert når dataene er ferdig bearbeidet.

Det er kun de som gjennomfører studien som vil få tilgang på opplysningene, overlege Derk Avenarius (UNN). Overlege Lil-Sofie Ording Müller (OUS) og Overlege Karen Rosendahl (Great Ormond Street Hospital for Children), vil se på bildene, **avidentifisert.**

Universitetssykehuset Nord Norge ved administrerende direktør er databehandlingsansvarlig.

Utlevering av materiale og opplysninger til andre
Hvis du og barnet sier ja til å delta i studien, gir du også ditt samtykke til at **avidentifiserte** bilder og **avidentifiserte** opplysninger utleveres Great Ormond Street Hospital for Children, London, England.

Rett til innsyn og sletting av opplysninger om deg og sletting av prøver
Hvis du og ditt barn sier ja til å delta i studien, har du rett til å få innsyn i hvilke opplysninger som er registrert om barnet. Dere har videre rett til å få korrigert eventuelle feil i de opplysningene vi har registrert. Dersom dere trekker dere fra studien, kan dere kreve å få slettet innsamlede prøver og opplysninger, med mindre opplysningene allerede er inngått i analyser eller brukt i vitenskapelige publikasjoner.

Økonomi og UNNs rolle
Studien er finansiert gjennom forskningsmidler fra UNN. Det er ingen økonomisk gevinst for UNN eller legene som gjennomfører denne studien.

Forsikring
Pasientskadeerstatningsordningen

Informasjon om utfallet av studien
Alle som deltar kan få informasjon om utfallet av studien dersom de ønsker det.

Samtykke til deltakelse i studien

Jeg er villig til å la mitt barn delta i studien

(Signert av foresatt, dato, sigenres uansett alder på barnet)

Deltakers navn, evt underskrift dersom barnet er over 12 år:

(Signeres også av barnet dersom barnet er over 12 år)

Jeg bekrefter å ha gitt informasjon om studien

(Signert, rolle i studien, dato)

Registreringsskjema håndleddsstudie del 2

Aksesjonsnummer……

Fødselsdato……..Kjønn M \ K

Tidligere
sykdommer:……
……
……
……

Medikamenter……
……

Høyde:…….
Vekt:…….
Sports
aktiviteter……
……trening……ganger per uke

H \V hendt

Traumer i siste tid?hva slags?.....
……..
hvor lenge siden?.....d\u\m

er du interessert i å delta i flere slike forskningsopplegg kan vi få lov å kontakte deg? …J \ N

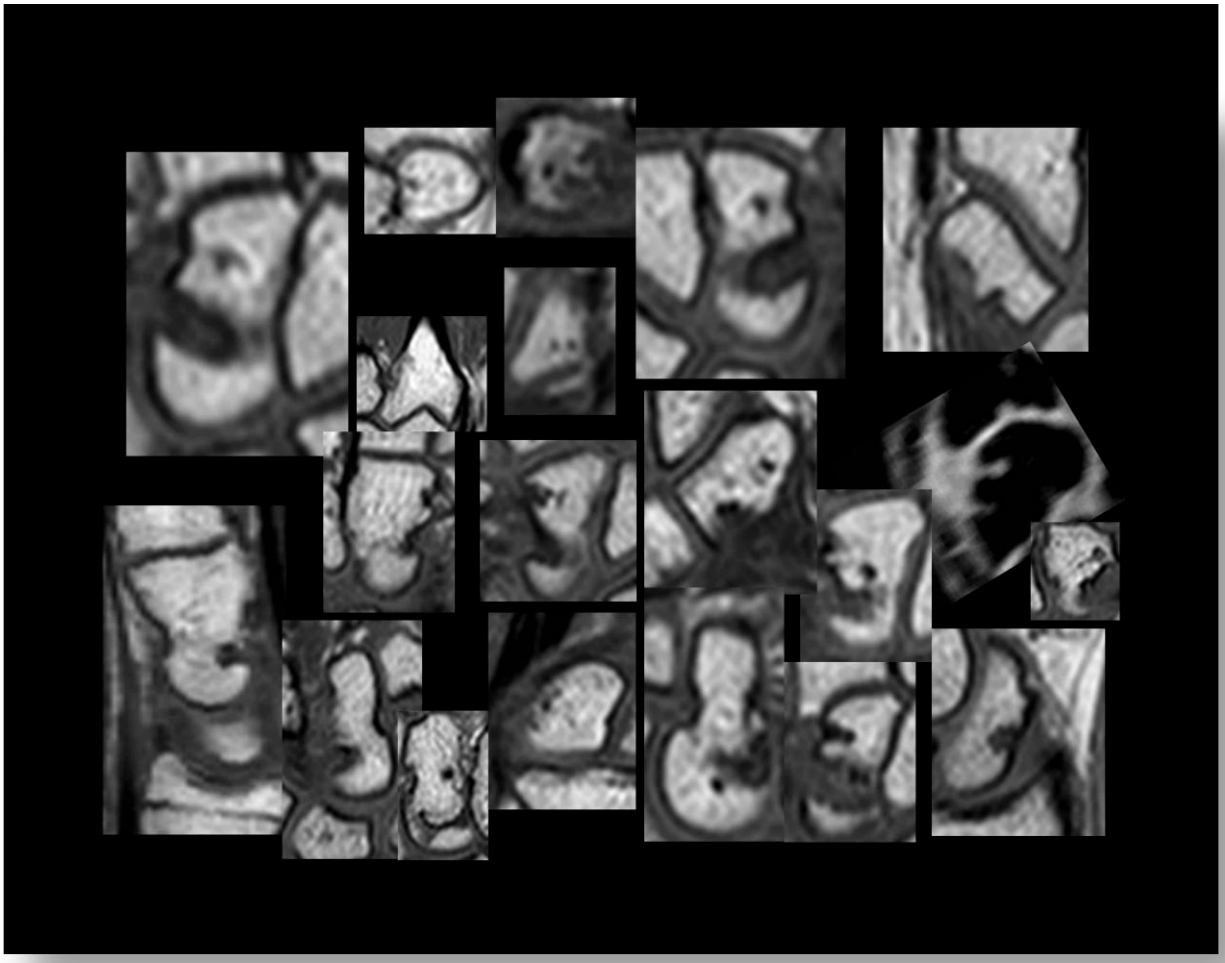

If you stare long at wrist bones, the wrist bones will also stare at you.

(free from Friedrich Nietzsche)